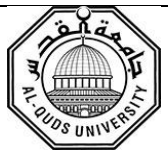

Joint mAster of Mediterranean Initiatives on renewabLe and sustainAble energy

Palestine Polytechnic University

Deanship of Graduate Studies and Scientific Research

Master Program of Renewable Energy and Sustainability

Islanding Detection Approach for Grid-Connected PV Inverter Using ANN Based DWT Technique

---

By

Haret Ibraheem Shalalda

Supervisor

Prof. Dr. Sameer Hanna Khader

Thesis submitted in partial fulfillment of requirements of the degree

Master of Science in Renewable Energy & Sustainability

March, 2020

The undersigned hereby certify that they have read, examined and recommended to the Deanship of Graduate Studies and Scientific Research at Palestine Polytechnic University and the Faculty of Science at Al-Quds University the approval of a thesis entitled:

"Islanding Detection Approach for Grid-Connected PV Inverter Using ANN Based DWT Technique"

Submitted by
Haret Ibraheem Shalalda

In partial fulfillment of the requirements for the degree of Master in Renewable Energy & Sustainability.

Graduate Advisory Committee:

Prof. Dr. Sameer Hanna Khader
(Supervisor). Palestine Polytechnic University
Signature: _____ Date: 2/11/2020

Dr. Fouad R. Zaro
(Internal committee member). Palestine Polytechnic University
Signature: _____ Date: 2/11/2020

Dr. Samer Alsadi
(External committee member). Palestine Technical University-Kadoorie
Signature: _____ Date: _____

Name: Prof. Dr. Murad Abu Sbeih
Dean of Graduate Studies and Scientific Research
Palestine Polytechnic University
Signature: _____
Date: 25-1-2021

Name: Prof. Dr. Wadie Sultan
Dean of Faculty of Graduate Studies
Al-Quds University
Signature: _____
Date: 17/10/2020

"Islanding Detection Approach for Grid-Connected PV Inverter Using ANN Based DWT Technique"

By **Haret Ibraheem Shalalda**

ABSTRACT

Islanding in electric power distribution system is a phenomena caused to the distribution generation when the main grid shuts down, or unintentionally because of grid blackouts, resulting in separated distribution generation working alone besides its local load. Due to safety and stability reasons, islanding should be early detected in order to disconnect the distribution generation.

Various types of islanding detection techniques have been applied and tested by researchers, like passive, active, and remote communication methods, all aimed mainly to minimize the non-detection zone at low power flow mismatch at the point of the common coupling. This study introduces islanding detection model for PV distribution generation inverter connected at the point of common coupling to real utility grid. The proposed islanding detection approach combines between the discrete wavelet transform technique, and the artificial neural networks (ANN).

A section of Hebron electric distribution grid that supplies the PPU campus has been tested at the point of common coupling with a standard model of PV inverter.

The proposed islanding detection method can continuously test the variations of grid parameters, mainly the voltage signals at the PCC was recorded during islanding and non-islanding events, then produced the discrete wavelet transform (DWT) in the form of energy content for each sample. The features function of detail coefficients was fed to ANN network in order to train it as pattern classifier to discriminate between islanding and non-islanding states.

Tested cases in this real grid-inverter connected power system showed high relative accuracy with average exceeded 94%, especially when events occur during low power flow between the main grid and the local load at the point of common coupling. The results achieved IEEE requirements for islanding regarding detection time period, and didn't affect the power quality of the system.

نموذج كشف الاستجزار لعاكس نظام شمسي متصل بشبكة كهربائية باستخدام الشبكة العصبونية الصناعية ANN ومحول الموجيات المتقطعة DWT

إعداد: حارث إبراهيم شلالدة

مُلخّص

الاستجزار Islanding هي ظاهرة تحدث عند انقطاع التيار عن نقاط الربط المتصلة بالعاكس في محطات التوليد والتوزيع الإضافية المتصلة بالشبكة الكهربائية، بحيث تبقى المحطة الفرعية في حالة عمل مستقلة وحدها تغذي الحمل المحلي. تؤدي هذه الظاهرة إلى الكثير من المحاذير والأخطار عند بقاء نظام الطاقة الإضافي في حالة عمل، حيث تؤثر على استقرار النظام، وأمان الشبكة والعاملين، لذلك يلزم إطفاء ذلك العاكس مُبكرا عند انقطاع شبكة الكهرباء الرئيسية.

لقد طُبّقت نُظم كشف متعددة عن حالة الاستجزار، منها الطرق الخاملة والطرق الفعالة، وتقنيات الاتصالات للكشف عن بعد. كانت تهدف جميعا إلى تقليل منطقة عدم الكشف في حالة الشبكة NDZ، والتي يتسبب فيها صغر قيمة تدفق الطاقة بين الشبكة الرئيسية والحمل المحلي. وأظهرت تلك الطرق نتائج متفاوتة في دقة الكشف والمدة الزمنية.

النظام المعتمد للدراسة والمحاكاة هو الخط المغذي لمبنى جامعة بوليتكنك فلسطين من شركة كهرباء الخليل، حيث يُقدم هذا البحث طريقة كشف عن الانقطاع يمكن اعتمادها في العاكس المحلي الموصول بمحطة طاقة فوتوفولتية. تتمثل الطريقة المقترحة بمُحاكاة حالات انقطاع الشبكة (الاستجزار) وحالات تغيرات طبيعية وتشويشات مؤقتة مثل أخطاء القصر الكهربائي بين الخطوط بأنواعها، وعمليات فصل ووصل الأحمال والمكثفات. تقوم هذه الطريقة على تسجيل إشارات الجهد، ثم إنتاج مُعاملات هذه الإشارت عن طريق محولة الموجيات المتقطعة DWT، واختبارها داخل شبكة عصبونية صناعية ANN بقصد تدريبها للتمييز بين حالات الانقطاع والحالات الأخرى.

نتجَ عن المحاكاة في هذا النظام العملي دقة عالية نسبيا في مختلف الأحداث التي تم تدريب الشبكة العصبونية عليها، خصوصاً في حالات تدفق الطاقة المنخفض بين الشبكة والحمل. وقد تجاوز معدل دقة التمييز في السيناريوهات المدروسة نسبة ٩٤%. بالإضافة إلى أن هذه الطريقة في الكشف لم تؤثر على جودة القدرة، كما أنها حققت متطلبات مؤسسة IEEE بحيث كانت فترة الكشف أقل بكثير من الفترة الزمنية المسموحة في الأنظمة المعمول بها في هذا المجال.

DECLARATION

I declare that the Master Thesis entitled:

"Islanding Detection Approach for Grid-Connected PV Inverter Using ANN Based DWT Technique"

is my own original work, and herby certify that unless stated, all work contained within this thesis is my own independent research and has not been submitted for the award of any other degree at any institution, except where due acknowledgement is made in the text.

Student Name: **Haret Ibraheem Shalalda**

Signature: Haret Date: 25.1.2021

STATEMENT OF PERMISSION OF USE

In presenting this thesis in partial fulfillment of the requirements for the joint Master's degree in Renewable Energy & Sustainability at Palestine Polytechnic University and Al-Quds University, I agree that the library shall make it available to borrowers under rules of the library.

Brief quotations from this thesis are allowable without special permission, provided that accurate acknowledgement of the source is made.

Permission for extensive quotation from, reproduction, or publication of this thesis may be granted by my main supervisor, or in his absence, by the Dean of Graduate Studies and Scientific Research when, in the opinion of either, the proposed use of the material is for scholarly purposes.

Any coping or use of the material in this thesis for financial gain shall not be allowed without my written permission.

Student Name: **Haret Ibraheem Shalalda**

Signature: Haret Date: 25.1.2021

DEDICATION

To my parents

To my wife and my children

To my brothers and sisters

To my faithful friends

To the martyrs souls

To our great Palestine

To the soul of poetry

&

Many thanks to every helpful person who support humanity

ACKNOLEDGMENT

First and foremost I would like to thank almighty God. I would like to show my gratitude to my family for their continued support, patience and encouragement over the years of my education. I greatly appreciate the thesis's supervisor Dr. Sameer Khader for his continuous support and time he spent with me in order to finish this thesis successfully. Many thanks to him also for his efforts as coordinator of the Master Program of Renewable Energy and Sustainability for all his guidance's and many thanks for all my teachers over the years of my education. Many thanks also to my colleagues in this master program.

I would like also to thank **JAMILA Project-544339-TEMPUS-1-2013-1-IT-TEMPUS-JPCR** funded by the European Union which was administrated by Sapienza University of Rome and partner Universities for their support in launching this program, provided infrastructure and opportunities for scientific visits.

LIST OF ABBREVIATIONS

RE	Renewable Energy
DG	Distribution Generation
PV	Photo Voltaic
MG	Micro Grid
PQ	Power Quality
IdM	Islanding Detection Method
PCC	Point of Common Coupling
ANN	Artificial Neural Network
MPPT	Maximum Power Point Tracking
DWT	Discrete Wavelet Transform
OVP	Over Voltage Protection
OFP	Over Frequency Protection
UVP	Under Voltage Protection
UFP	Under Frequency Protection
THD	Total Harmonics Distortion
PLL	Phase Locked Loop
AFD	Active Frequency Drift
ROCOF	Rate of Change of Frequency
SFS	Sandia Frequency Shift
SVS	Sandia Voltage Shift
SMFS	Slip Mode Frequency Shift
SCADA	Supervisory Control and Data Acquisition
HPF	High Pass Filter
LPF	Low Pass Filter
FFPB ANN	Feed Forward Back Propagation Artificial Neural Network
SCG	Scaled Conjugate Gradient
PPU	Palestine Polytechnic University
IEEE	Institute of Electrical and Electronics Engineers

LIST OF FIGURES

LIST OF TABLES

TABLE OF CONTENTS

CHAPTER 1

1. Introduction

1.1 Overview

In traditional electrical power distribution networks, there are main generation stations and distribution generation substations supporting each other to cover the basic load, and also any upgraded sections of future rising loads.

Fortunately, the presence of micro grids (MG) in parallel with the main network can enhance power distribution stability and reliability, and share a part of the load in critical situations. On the other hand, connection of theses micro grids could be harmful to overall system, basically the main parameters of both networks; voltage, frequency must match and remain stable. Once the utility grid turns off, local micro grid might not fulfill the local load due to different possible reasons, therefore, the system goes under malfunctioning unstable operation, so this situation should be detected early to disconnect it directly [1], [2].

Moreover, disconnection of the DG guarantees the safety of the humans and equipment's, where sometimes the electrical distribution company maintenance staffs could expose to electric hazards while they are trying to follow and fix the fault.

1.2 Renewable Energy Distribution Generations

Recently, fast spread of renewable energy resources; PV, wind turbines, and others, RE distribution generations or micro grids have become a significant part of the main grid. Renewable DG's are connected to the grid at the point of common coupling (PCC) through inverters which flow the energy into the main grid. The DG's have their own management, protection, control, and monitoring systems [3]. Since there is continuous fluctuation in the power produced from these RE stations, the power flow between the grid, DG, and load is continuously changing even if the local load is constant. Therefore, when the grid is shut down, the inverter must turn off also to avoid this risky situation on system parameters stability [4].

1.3 Islanding Phenomena

Unintentional islanding is a phenomenon occurs when the utility grid shuts down due to electric faults, hence the distribution generation DG continues its operation supplying the local load connected at PPC as shown in Figure 1-1, and becomes as an isolated island within the rest of the network. Due to safety reasons for the system and operators the DG inverter must turn off as early as possible [5].

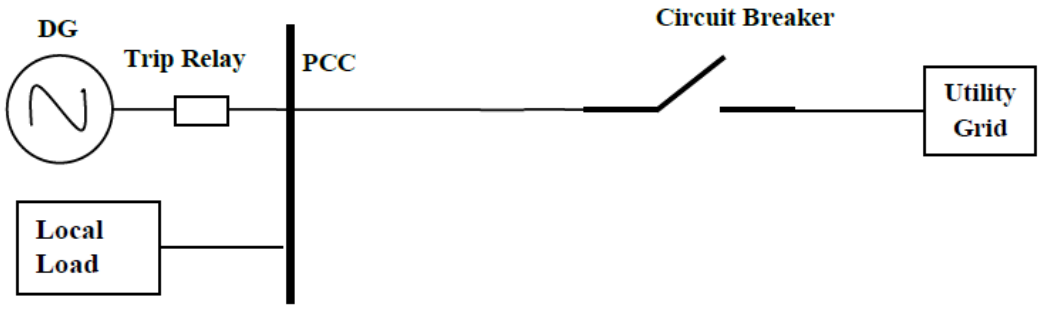

Figure 1-1: DG station behavoiur during islanding

1.4 Anti-islanding Standards and Regulations

Interconnection between the DG and the utility grid becomes the most critical when the power flow mismatch becomes large, at that condition, when the grid turns off due to any fault or operation reason, the produced power from DG couldn't fulfill the load requirements, this will cause abnormal situations at the PCC voltage and frequency, which must not last more than 2 seconds according to IEEE 1547 standards [6].

Table 1-1 and Table 1-2 show the allowed interconnection response time periods for different ranges of voltage and frequency variations, respectively, in terms of the number of voltage cycles started from the event occurrence moment.

Table 1-1: 1547 IEEE standard for abnormal voltage during islanding [1]

Voltage Range (% of the base voltage)	**Clearing time (s)**
V < 60	0.16
60 ≤ V < 106	2
106 ≤ V < 132	Normal operation
132 ≤ V < 144	1.0
144 ≤ V	0.16

Table 1-2: 1547 IEEE standards for abnormal frequency during islanding

DG size	**Frequency Range (Hz)**	**Clearing time (s)**
≤ 30 kW	> 60.5	0.16
	< 59.3	0.16
> 30 kW	> 60.5	0.16
	< {59.8 to 57.0} (adjustable to set point)	Adjustable 0.16 to 300
	> 57	0.16

1.5 Islanding Detection Methods

There are different types of islanding detection methods where researchers categorize them into four main classifications [2] as listed in .

1. Passive islanding detection techniques
2. Active islanding detection techniques
3. Hybrid islanding detection techniques
4. Remote islanding detection techniques

stating the most common and applied islanding detection methods.

Table 1-3: Islanding Detection Methods

Passive Islanding Detection Techniques	Active Islanding Detection Techniques	Remote Islanding Detection Techniques
- Under/Over Voltage (UOV), and Under/Over Frequency (UOF) method - Voltage Phase Jump Detection (VPJ) -Voltage and Current Harmonic Detection.	-Sandia Voltage Shift (SVS) -Sandia Frequency Shift (SFS) -Slip Mode Frequency Shift (SMFS) -Frequency Jump (FJ) -Rate of Change of Frequency (ROCOF) -Detection of Impedance at Specific Frequency. -PLL based active method -Active frequency drift (AFD)	-Transfer Trip Scheme -Power Line Carrier Communication (PLCC) -Impedance Insertion

Through wide investigations in researcher's publications in the field, mostly applied islanding detection methods are the following:

1. **Over voltage and under voltage OUV, over frequency and under frequency OUF protection:**

   In this method, the islanding detection monitors the PCC voltage and frequency, threshold values are pre-set to activate relays to disconnect the inverter below minimum values of voltage and frequency and beyond maximum values within the allowed detection time according to the IEEE standards [6]. In chapter 2, the author introduces more demonstration about this method with relation to P-Q model and power flow interaction between grid, load, and inverter.

2. **Phase jump detection**

First of all, the voltage phase at the PCC is forced by the system (main grid), once the grid disconnects from the PCC, and as the current of the current source inverters (CSI) behave as reference, as demonstrated in Figure 1-2, the voltage phase jumps from its previous state before islanding to a new point in the next zero crossing to follow the inverter current phase, hence this phase difference is used to identify islanding. Despite VJD method has simple implementation, it is difficult to choses the proper thresholds since it depends on the installation site [1].

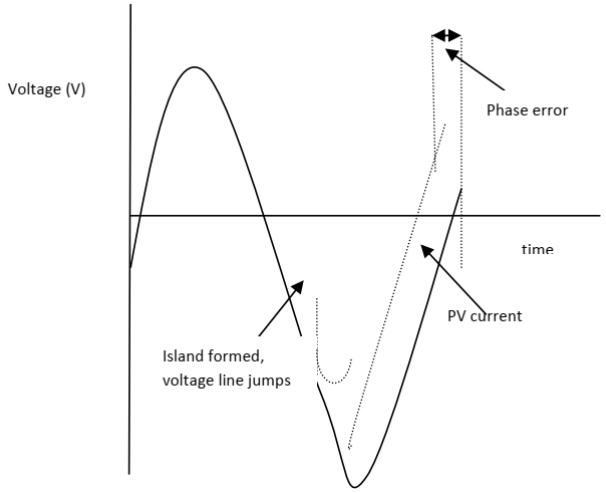

Figure 1-2: Phase jump islanding detection operation [1]

3. **Detection of harmonics**

In this method, DG inverter measures the voltage total harmonics distortion at the PCC, and compares it to threshold value to disconnect itself. Once the grid fails, the THD of load circuit well increase since the impedance of local circuit is higher than grid impedance. Harmonic detection method is effective and secure, but it requires careful selection of threshold value of the THD [4].

4. **Rate of Change of Frequency**

When the grid is lost, the power imbalance at the PCC causes the frequency to deviate within a time period, by monitoring this df/dt and comparing it to pre-set threshold islanding detection is decided and trip signal disconnects the inverter. According to [4], the allowed detection time period for ROCOF method is accepted between 4-6 cycles.

5. Sandia Voltage Shift

The method is applied by adding positive feedback to the inverter voltage amplitude, when the grid is no more connected, the PCC voltage reduces significantly, and islanding decision takes place and disconnects the UVP relays [3]. The SVS method is effective and don't affect power quality of the power system.

6. **Sandia Frequency Shift**

The SFS is performed by applying positive feedback to the voltage system frequency causes the frequency to change whenever islanding event occurs, as a result, and when the system phase angle changes out of pre-specified threshold, then islanding is detected and UFP relays trip the inverter [3].

7. Impedance Insertion

When there is primary indication on islanding occurrence, adding low capacitive impedance inside the island will change the phase and decrease the frequency accordingly, then the under frequency protection relays disconnect the inverter permanently. This method is expensive since it requires extra installations on the grid side, and it has slow response [1].

8. Remote Islanding Detection Methods

These methods requires interactive communication systems between utility grid side and distribution generation side. In power line communication method, there is continuous low voltage signal flows through the power line from transmitter in the grid side to a

receiver in the inverter side as shown in Figure 1-3, when this signal is lost, then the inverter disconnects within a pre-defined time period to avoid islanding situation.

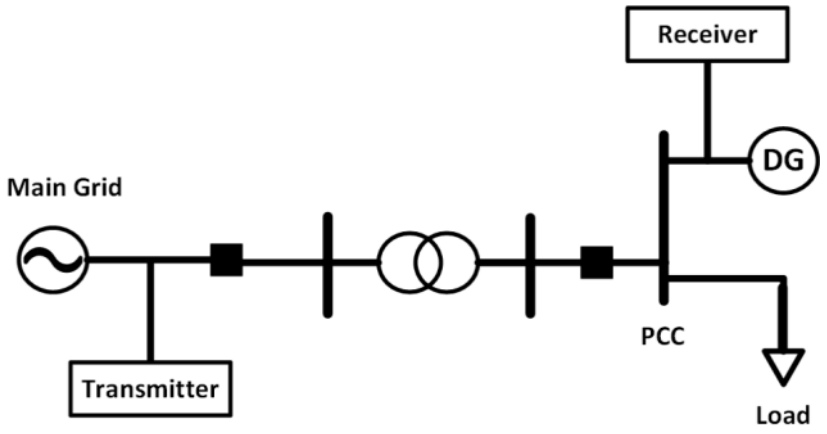

Figure 1-3 :Remote islanding detection scenario

Also SCADA method, and transfer trip method are used. By continuous monitoring of power distribution system parameters and switching devices, it is easy to transfer a trip signal to any DG connected to the grid in case of islanding. In general remote detection methods are reliable and efficient, and perform the detection with very small NDZ. On the other hand, they are costly and risky in case of communication failure.

1.6 Methodology

Basically, the researcher proposes to build the islanding detection approaches independently, and then to find out the parameters area (within threshold range) of each method that specify the happening of islanding. Consequently, finding where these areas overlap as most as they emphasize the final decision of the monitoring system.

To do so, optimization method is required, so by applying intelligent algorithm; like artificial neural network (ANN) that computes iteratively the optimized data set to insure islanding condition.

Continues learning process during operation can save the most important data, and can be used later to determine islanding occurrence for similar (or closer) status in terms of system parameters at the PCC. As time passes, the results enhance system capability for correct and accurate decision resulting in powerful and robust detection algorithm.

From signal processing pint of view, discrete wavelet transform (DWT) is one of most applied and powerful methods; the power, voltage and current waveform can be analyzed to detect any disturbance and critical changes in the main parameters that describe its own status.

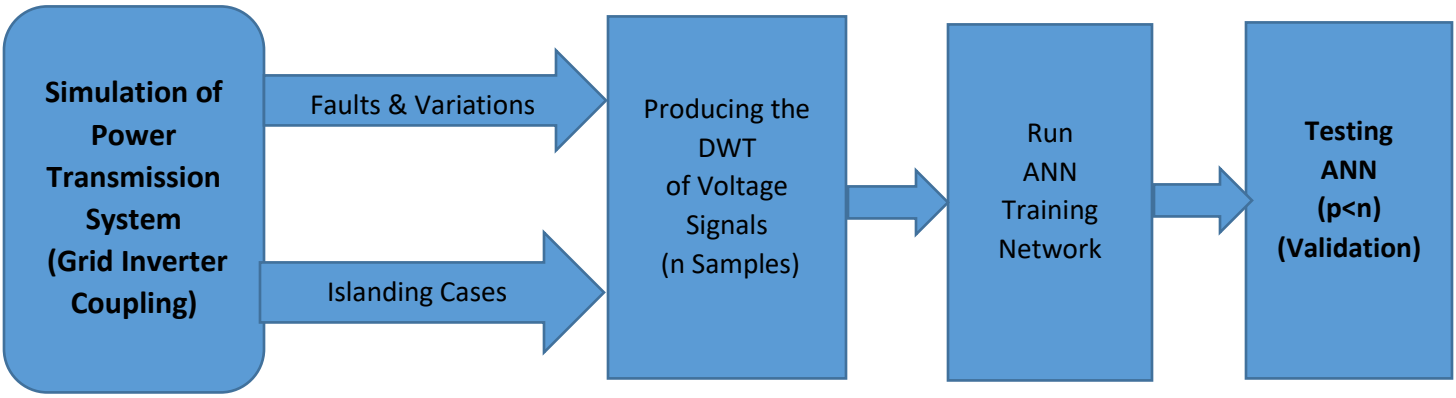

Figure 1-4: Thesis Methodology flowchart

1.7 Scope of the Study

The following objectives are the foundations of this research

- To simulate the power distribution system coupled with the PV inverter using MATLAB/SIMULINK in different loading cases under islanding conditions and fault conditions for n-samples.
- To generate the DWT of those signal samples as feature function contains of detail and approximation coefficients.
- To find the suitable artificial intelligent network and train it to discriminate between islanding cases and other grid normal and fault cases.
- Training the ANN at different DWT decomposition types in purpose to determine the best DWT type that describes the system behavior accurately.
- To find out the optimal and minimum number of power voltage cycles enough to detect the islanding situation.

1.8 Thesis Structure

This thesis is structured in five chapters after the introductory sections from the abstract to acknowledgement; chapter one introduces the main concepts and theoretical background about the islanding, and illustrates clearly the thesis scope and methodology. Chapter two presents a literature review discussing previous researches and makes a comparison between papers results which were published in the field of study. In Chapter three, the author builds the three models of his suggested approach; power system model, DWT model, and ANN model. The Simulation results of the three interconnected systems are presented and discussed in chapter five, while chapter six finally summarizes and evaluates the model in terms if it's results and conditions, and introduces authors conclusions, recommendations, and suggested future work.

CHAPTER 2

2. Literature Review

2.1 P-Q Model and Non-Detection Zone

Voltage profile and electric grid voltage frequency are affected mainly by active and reactive power flow behavior between the power system units, traditional generation stations, RE distribution generation, and loads, therefore any change in power flow is followed by corresponding change in system voltage and frequency [7], [8].

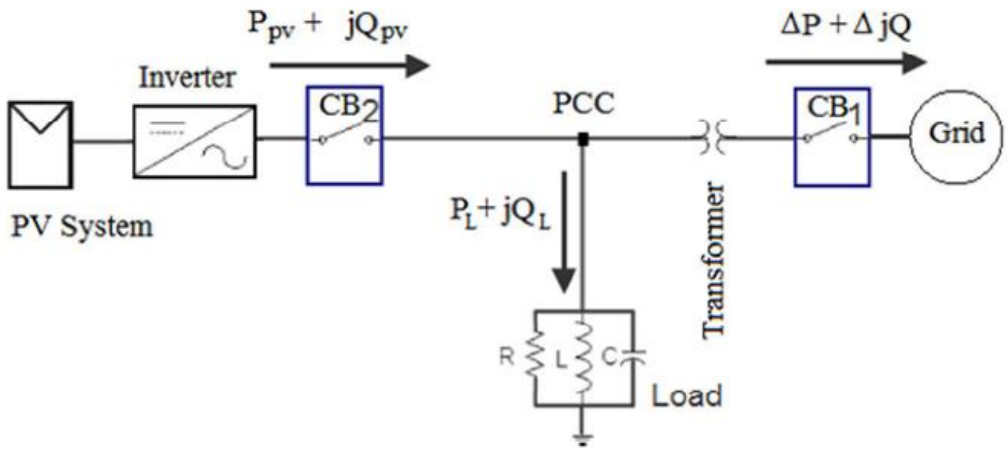

Figure 2-1: Power flow of grid-DG-load connected system

Since the power flow on the PCC as shown in Figure 2-1 is the most effective factor of the system stability, and by direct monitoring upon the voltage and frequency, it will be noticed that in case of ΔP and ΔQ are huge values, then islanding situation will be detected easily because the utility grid shut down necessary causes big changes in V and f, where over and under voltage relays OUV and over and under frequency OUF relays are used in [7], [9]. On the other hand, in case of small ΔP and ΔQ, the variation in V and f is small and still within the system normal acceptable variations. This grey area of voltage and frequency window is

called the non-detection zone (NDZ), and islanding couldn't be easily and accurately detected or confirmed using passive islanding detection methods. P-Q model procedure leads to the most interesting equations below which limit the window of V and f in P-Q frame [10], [11].

$$P_{load} = P_{DG} + \Delta P \quad \text{……} \quad \text{(2.1)}$$

$$Q_{load} = Q_{DG} + \Delta Q \quad \text{……} \quad \text{(2.2)}$$

$$Q_f\left(1 - \left(\frac{f}{f_{max}}\right)^2\right) \leq \frac{\Delta Q}{P_{DG}} \ll Q_f\left(1 - \left(\frac{f}{f_{min}}\right)^2\right) \quad \text{(2.3)}$$

$$\left(\left(\frac{V}{V_{max}}\right)^2 - 1\right) \leq \frac{\Delta P}{P_{DG}} \ll \left(\left(\frac{V}{V_{min}}\right)^2 - 1\right) \quad \text{……} \quad \text{……} \quad \text{(2.4)}$$

Where Q_f is the quality factor, P_{DG} and Q_{DG} are DG inverter active and reactive power respectively, V_{max} and V_{min} are OUV thresholds of the NDZ, f_{max} and f_{min} are OUF thresholds of the NDZ as shown in Figure 2-2 below.

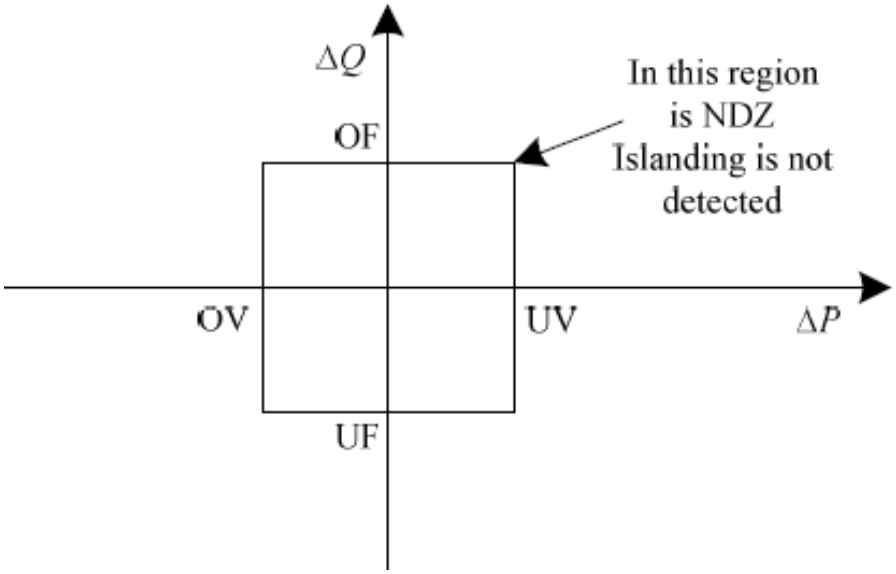

Figure 2-2: None detection zone in terms of V and f

2.2 Passive and Active Islanding Detection Method

Passive and active islanding detection methods try to test and utilize the system parameters at the PCC such as voltage, frequency, and power flow. Passive islanding detection methods measures that variations occur when any event takes place suddenly, and take a decision depending on threshold limits during the event location and time period [2], [5]. Unfortunately, the non-detection zone is quite large due to the problem of low power flow that could happen when the load power is very close to DG inverter generated power; at this case, grid disconnection doesn't affect the parameters at the PCC sufficiently to detect any event; fault, or even islanding as well that happens at all. Unlike passive methods, active islanding detection methods improve NDZ, and response time [7]. On the other hand, they reduce the power quality of the system, because these methods are based on external signal injection into the power grid. Therefore, active method still has the advantage because they don't affect the power quality and system parameters at the PCC [5].

In [11], passive and active methods have been simulated; Over/under voltage and over/under frequency method, phase locked loop based method, and active frequency drift (AFD). In the results, the detection time in was shortened, but the frequency change needed large power mismatch between DG and load, with purpose to trip the protection relays of anti-islanding control system.

One of the effective islanding detection method is slip mode frequency shift (SMFS) applied in [8] on a single phase PV inverter, the attention of the study was towards system frequency stability during islanding situation.

Reactive power control method adopted in [14] depended on voltage deviation caused by ΔP, and frequency deviation caused by ΔQ changing at PCC during any event. The simulation achieved small NDZ in power mismatch cases, and shortened the detection time for high X/R grid lines. On the other hand, it didn't present convinced results for small ΔP and ΔQ.

One of the most applied passive methods is the rate of change of frequency (ROCOF) proposed in [15], the study results showed narrower NDZ window bounded with smaller margin of

frequency thresholds compared to over and under frequency protection method (OUFP). Furthermore, the active method in [16], the author monitored the voltage harmonics on the PCC, and used to adjust the inverter reference power in order to monitor the behavior of the system voltage as a result of power flow change. This power injection method is effective but unfortunately affects the power flow and power quality, and disturbs the voltage at the PCC.

2.3 Recent Intelligent Islanding Detection Research's

Distribution generation systems connected to the main utility grid have increased the complexity of the system normal operation, and more, mal operation conditions necessarily. Traditional solving computational models have been used to control and monitor power systems tell few years ago became weak and ineffective. Therefore, researchers proposed many intelligent techniques to detect islanding, they depend on intelligent iterative algorithms, and artificial networks, rather than system normal equation solvers, which can be applied only on linear and simple systems.

Recently, artificial and intelligent algorithms, like artificial neural networks (ANN), particle swarm optimization (PSO), and others have been widely used in power systems.

The author in [17] proposed the non-dominated particle swarm optimization technique for islanding scheme in a distribution system. ANN-PSO proposed in [18] tried to make use of minimum features of the grid-inverter parameters to detect islanding events through feature function contains ΔP, ΔQ, and df/dq, and achieved acceptable classifying performance.

In [10], the authors proposed islanding detection approach by employing the DWT as feature extraction tool for passive detection method; over under voltage and frequency technique. Although they achieved fast and power quality friendly method, the NDZ still large.

CHAPTER 3

3. Modeling

3.1 Power System Modeling

3.1.1 Distribution System Description

Palestine Polytechnic University (PPU) campus in Hebron / Palestine is fed from 33kV medium voltage feeder through 33kV/11kV transformer, as shown in Figure 3-1 below, where the system components ratings, and operation parameters are listed in Table 3-1.

Table 3-1:Distribution Power System Components

Type	Power Component	Specifications	Remarks
Transformers	Transformer 1	33/11 kV, 13 MVA	
	Transformer 2	11/0.4 kV, 1000 kVA	
	Transformer 3	11/0.4 kV, 400 kVA	
	Transformer 4	11/0.4 kV, 1000 kVA	PPU load transformer
Loads	Load 1	470 kVA	
	Load 2	400 kVA	
	Load 3 (PPU)	355 kVA	(PCC)
Distribution Lines	Line 1	1500 m	
	Line 2	235 m	
	Line 3	150 m	
	Line 4	200 m	

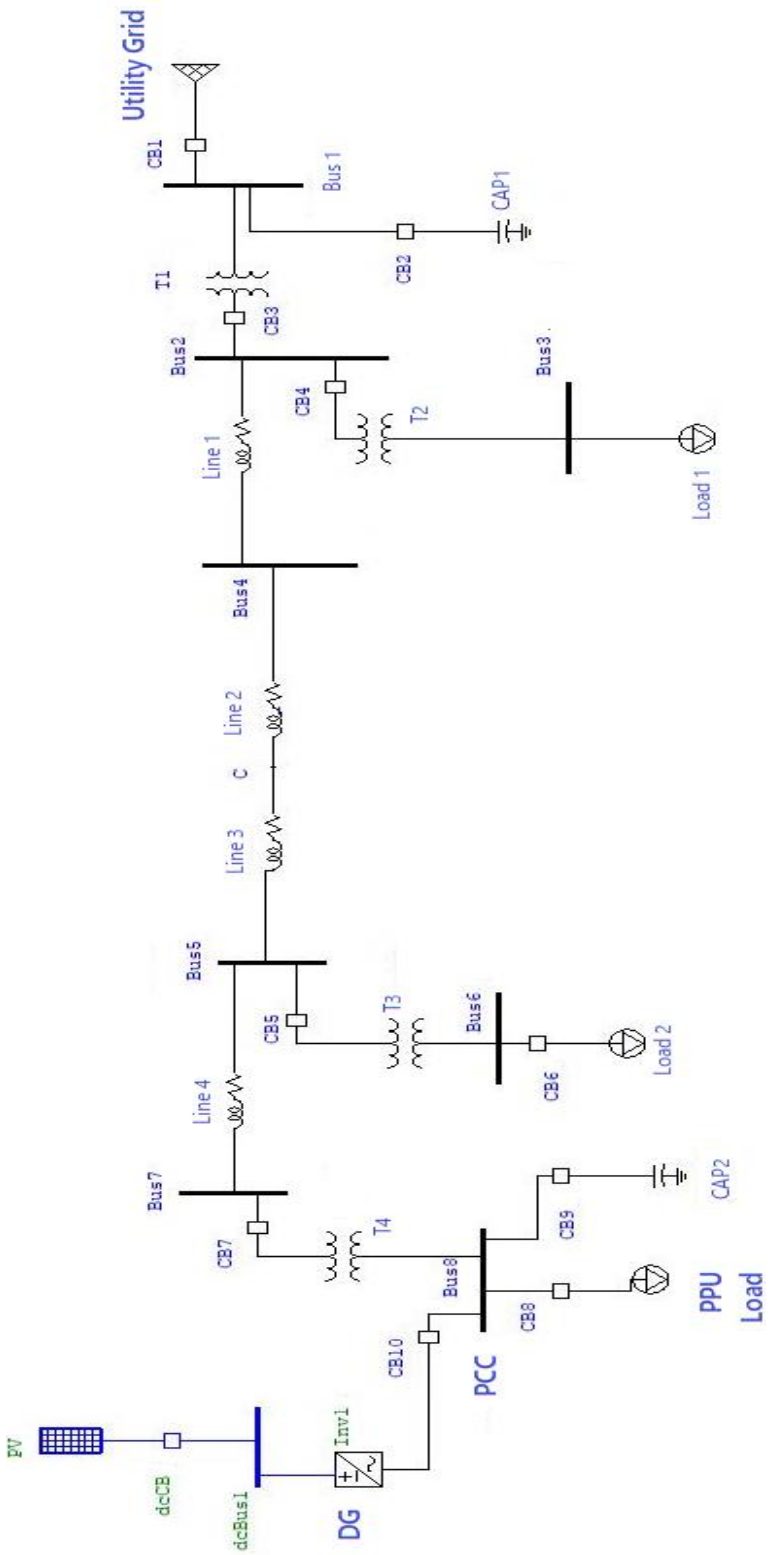

Figure 3-1: Tested power distribution system

The main feeder of the utility grid is 33kV, and the X/R ratio of the source equals 10, and the impedances of the four sections of the power distribution lines are:

Line section 1: 0.204 + 0.15j Ω

Line section 2: 0.024 + 0.0175j Ω

Line section 3: 0.037 + 0.028j Ω

Line section 4: 0.032 + 0.023j Ω

3.1.2 **Grid-Inverter Connection**

The Electric load of PPU buildings PV inverter is connected to the distribution lines grid supply through PV inverter as a distribution generation station. By this coupling at the output of 1MVA transformer, the research aimed to test islanding detection at low voltage scale (400 V) as illustrated in Figure 3-2.

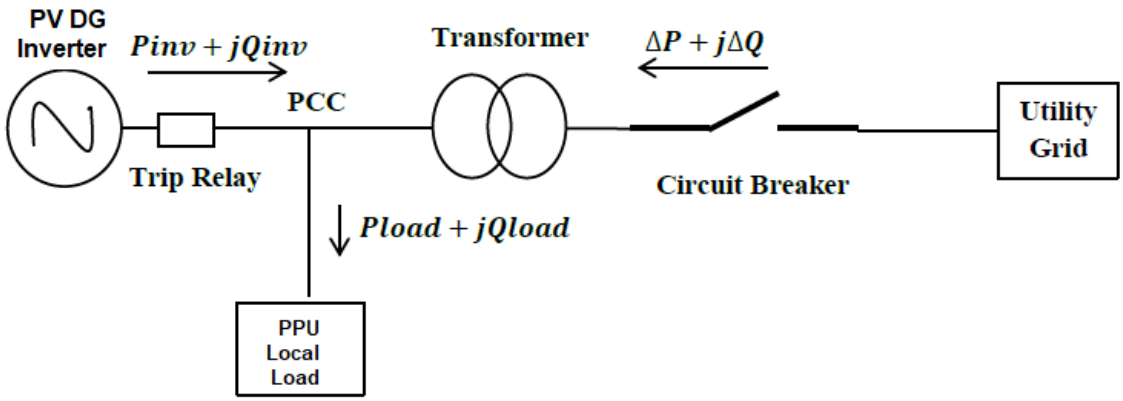

Figure 3-2: Grid-DG-Load operation

Figure 3-3 shows the PV-based distribution generation system feeds boost converter which is connected to 3 phase inverter provided of maximum power point tracking (MPPT) controller. Basically, the main system component parameters are:

- 200 kW_p power PV array produces 273 V from 128 parallel strings each of 5 series modules.
- Boost converter switched with 5 kHz control frequency with output DC bus voltage: 700 V, controlled by MPPT system.
- The 3-leg bridge inverter outputs 400 V line to line 3 phase voltage, and connected to the utility grid through line inductor.

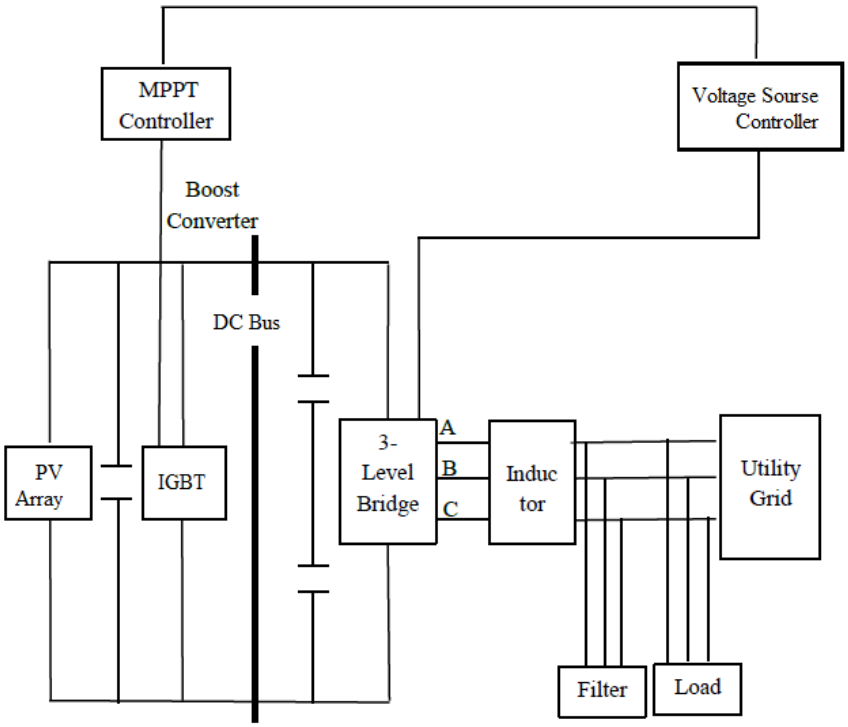

Figure 3-3: PV DG inverter connected to load-grid coupling

3.1.3 Faults, and Islanding Events

In this study, the researcher proposed 140 different grid abrupt events cause system disturbance at PCC, they are mainly divided into two categories; islanding, and non-islanding events as listed in

Table 3-2. These cases well be simulated at different loading and ΔP, certain attention is given to situations of small ΔP when the load is almost supplied from the inverter.

Table 3-2: Simulation samples of power distribution system disturbance cases

Islanding Cases	Non-islanding Cases		
	Faults	Load Variations/Switching	Capacitors Switching
64	53	11	12

3.2 Discrete Wavelet Transform Modeling

3.2.1 DWT Theory in Power Systems

Theory of wavelet transform is being applied in wide range of power systems researches, such as faults detection, power quality studies, de-nosing power signals, and extraction of power system features [7], [19]. DWT can produce very effective and accurate data about the power system, and it can describe the high frequency content and changes that couldn't be identified using traditional methods. By analyzing voltage or current waveform in terms of their details, then the image will be very clear, hence it will be easy to distinguish between normal grid-load variations, or acceptable operation faults, and islanding cases that need trip decision from the control system.

3.2.2 Selecting DWT Mother Wavelet

Mostly, in power systems applications, Daubechie's family mother wavelet approaches for decomposition of power signals analyzing has been commonly applied in [19], [20], where it worked efficacy and accurately. Hence, Daubechie 4 (db4) shown in Figure 3-4 is selected as the main mother-wavelet in this study analysis since it showed good compactness in power systems research.

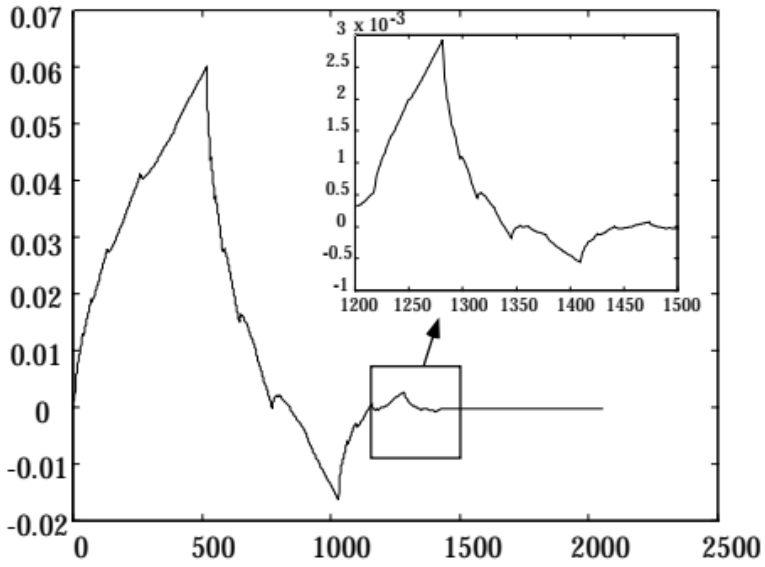

Figure 3-4: Daubechie's mother-wavelet [21]

Discrete wavelet transform of signal function f(k) is defined as:

$$DWT_{\varphi}\, f(m.n) = \sum_{K} f(k)\varphi^{*}{}_{m.n}\,(k) \tag{3.1}$$

The mother wavelet is:

$$\varphi_{m.n}(k) = \frac{1}{\sqrt{a_0^m}}\ \varphi\left(\frac{k - n b_0 a_0^m}{a_0^m}\right) \tag{3.2}$$

Where $a_0 > 1$ and $b_0 > 0$, and m and n are positive integer numbers [20].

The m-level approximation coefficient, and m-level detail coefficient of the waveform as in equations (3.3) and (3,4) below [20].

$$a_m\,(n) = \sum_{n=1}^{N} g(2n-k)a_{m-1}\,(k) \tag{3.3}$$

$$d_m\,(n) = \sum_{n=1}^{N} h(2n-k)d_{m-1}\,(k) \tag{3.4}$$

Approximation coefficient a_1 represents the RMS value of the phase voltage, and the feature vector [d_1, d_2, …, d_n] represents the detail coefficients of the voltage signal harmonics caused by transient behavior which increase clearly during abrupt changes and system parameters variations.

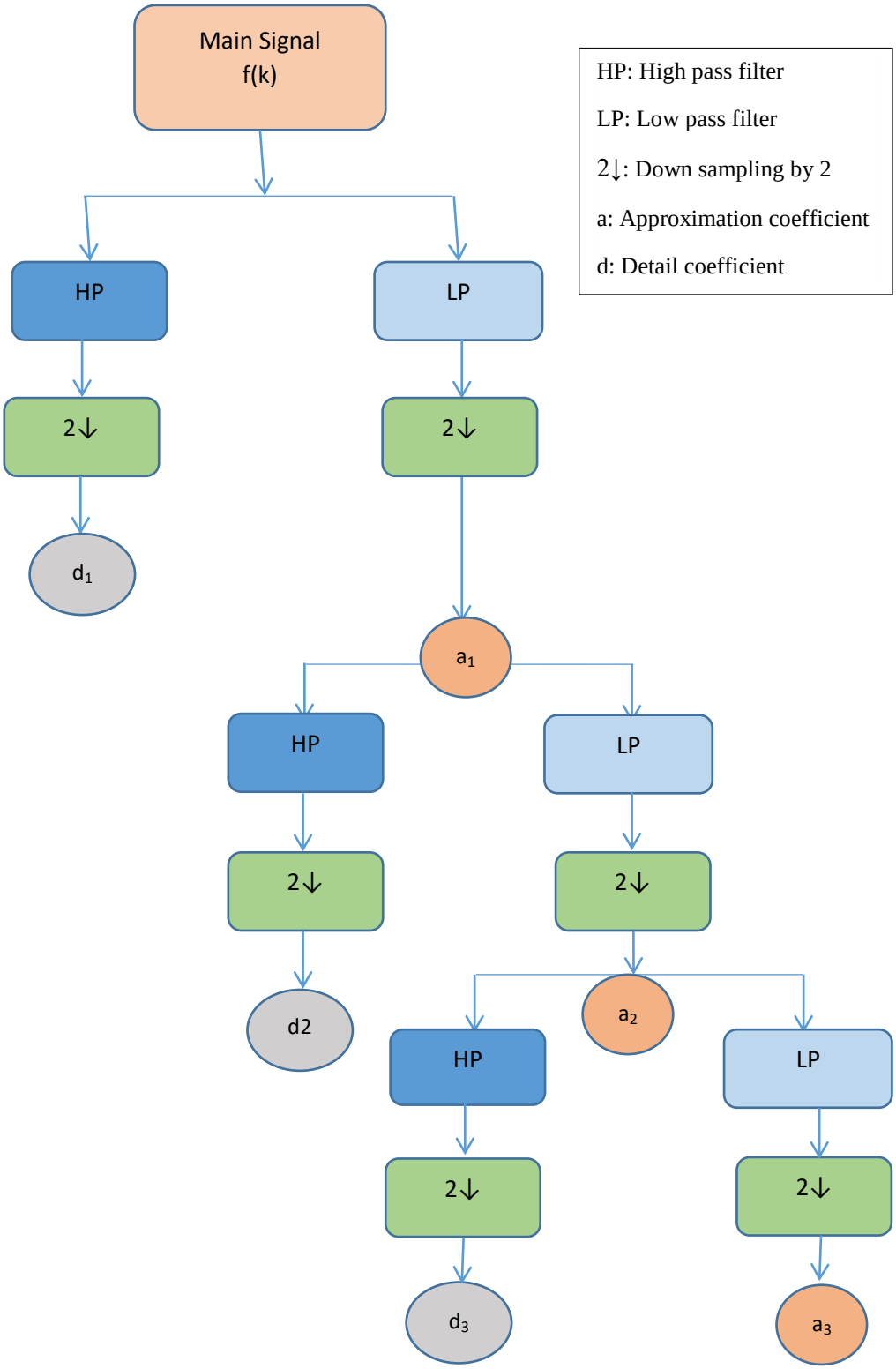

Figure 3-5: DWT of three level details decomposition

In this study, the voltage signal has been decomposed to 5 levels of details, where the DWT sampling frequency was selected to be 5kHz, hence, the details frequencies for all decomposition levels during down sampling are shown in Table 3-3, where each level has half the frequency of the previous one.

Table 3-3: Frequencies of DWT levels

Detail Level	Frequency
1st level	5000 Hz
2nd level	2500 H z
3rd level	1250 Hz
4th level	625 Hz
5th level	375.5 Hz

In this case, and according to Shannon's theorem [22], as shown in Figure 3-6, the maximum frequency can be captured is 5 kHz.

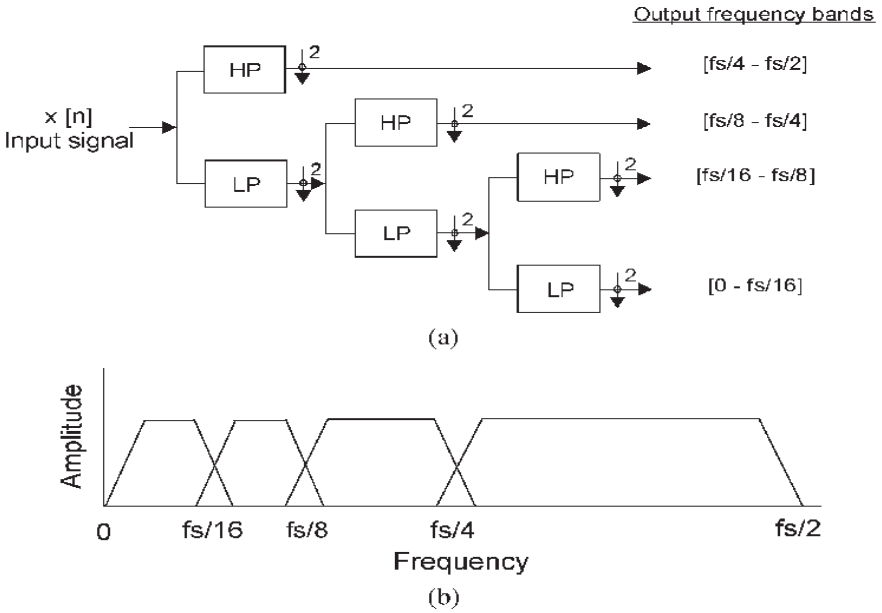

Figure 3-6: Signal down sampling frequencies (a) DWT sampling by LP and HP filters (b) Filter band for each frequency.

3.2.3 Energy Density Method Based DWT

To find the feature vector that describe every event happens at the PCC using the concept of discrete wavelet transform, some approaches, like relative spectral energy method have been applied in [22]. Threshold value is set to comprise between islanding and other cases. This could give misleading information since that some high disturbance could last very short time, as a result, the monitoring system may output wrong decision.

The proposed method in this study applied the energy density content method in [23]. Equation (3.5) is used to calculate the parameters of the feature vector produced by the DWT. Energy density content adopted in [23] guarantees sufficient high value in the disturbed cycle when an event occurred.

$$E_p = \sqrt{\sum_{i=1}^{N} \frac{(abs\,(d_p\,(i)))^2}{N}} \tag{3.5}$$

Where E_p, is the energy content in phase p (a, b, or c), N is the number of detail coefficients in each level of decomposition, and $d_p\,(i)$ represents the i-th confident in each detail of the phase voltage. Therefore, the three phase feature vector (F) of five levels decomposition becomes:

$$F = \{D_1,\ D_2,\ D_3,\ D_4,\ D_5\} \tag{3.6}$$

Where each detail of them ($D_1\ to\ D_5$) represents the total energy density in the corresponding sub detail of the three phases, E_{ip}.

In some way, for each event voltage sample, the feature vector components form the deterministic characteristic of the event depending on the nature of that event, location on the network, and also on grid conditions, like grid power component parameters, and active and reactive power flow at the PCC. Therefore, this one input matrix with its corresponding output are introduced to the ANN to learn by training itself on the 140 samples. Not only the relative values of ($D_1\ to\ D_5$) describe the event characteristic, but also the pattern in which they are arranged in the matrix.

3.3 Artificial Neural Network Modeling

3.3.1 Artificial Neural Network Overview

Nowadays, complex technology produces large amount of data which statically requires non-traditional intelligent classification methods. Artificial neural networks was inspirited from human brain operation and data transfer between neurons [24]. Human brain and neuron system can remember and classify any event or image or data of any shape by self-learning through weights stored from previous experience, and by continues learning, it utilizes this experience to distinguish any upcoming similar event, image, or data. ANN function in brief, is to relate a set of inputs to its corresponding features output.

3.3.2 Artificial Neural Network Operation

In addition to the input set and network output, and for single neuron network as shown in Figure 3-7, ANN basically is built from the nodes which gather the inputs, multiply them by their weights and then, transfer them through neurons to nonlinear sigmoid function like tangent function to produce the output Y_o. For each set of inputs, the dynamic network continues adjusting weights until it reaches the higher possible accuracy of classification.

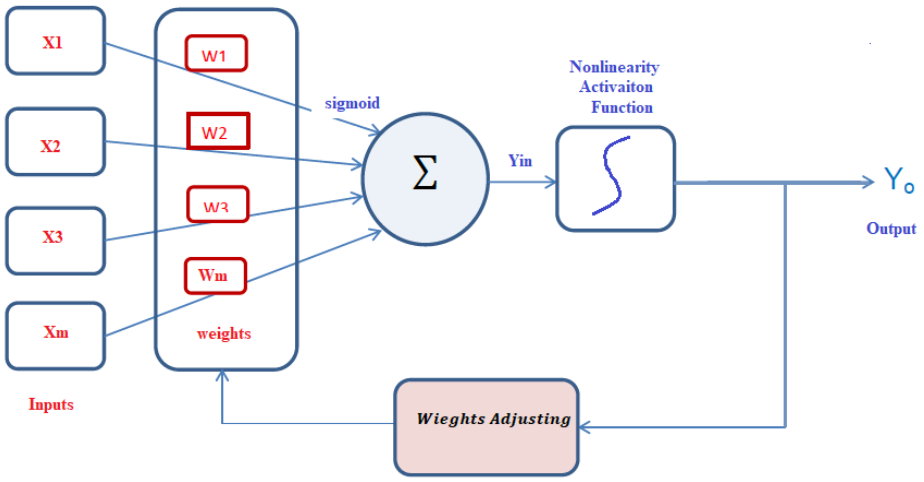

Figure 3-7: ANN general principle of operations

Equations (3.7 – 3.8) describe the simple operation of the network.

$$Y_{in} = w_1 * \boldsymbol{x_1} + w_2 * \boldsymbol{x_2} + \cdots + w_m * \boldsymbol{x_m} \tag{3.7}$$

$$Y_o = F(Y_{in}) \tag{3.8}$$

Where x refers to the input, and w refers to corresponding weight. Y_{in} is the summation at the node, and Y_o is the final output of the network.

While some systems learn using one layer, other systems require more sophisticated networks, so, one or more hidden layers could be added as shown in Figure 3-8. Multilayer networks definitely increase the learning time of the training and requires processors of higher specifications.

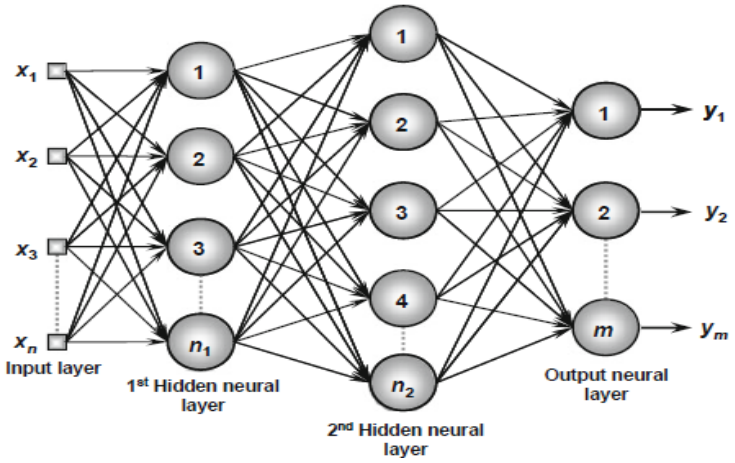

Figure 3-8: Example of a feed forward network with multiple layers [15]

3.3.3 Selected Feed Forward Back Propagation ANN

In general, artificial neural networks can learn during the training, but some networks are more dedicated and fit for data type system. Many factors influences the progression of learning; input matrix size and there dependence on each other, number of hidden layers, sigmoid weights, and the type of activation function. Feed Forward back propagation (FFBP) network is mostly used in power system applications, with minimum hidden layers it takes shorter time to learn. Adopted network in this research (FFBP) has the following main parameters:

- Training function: updates weight and bias values according to the scaled conjugate gradient (SCG) propagation method, it consumes less training time according Moller [25].
- Input: one matrix of DWT coefficients feature vector.
- Layers: 2 layers.
- Bias: 2 weight bias arrays.
- Neurons: 40-1000, change upon simulation results training regression.
- Output: one output

.

CHAPTER 4

4 Simulation and Analysis

4.1 Introduction

According to the approach modeled in the previous chapters, the three subsystems have been simulated using MATLAB/SIMULINK, where the distribution grid-DG inverter subsystem results (islanding and non-islanding samples) form the input raw data of the second subsystem (DWT) to produce the feature vector as the input of back propagation feed forward artificial neural network BPFF ANN, this third subsystem is aimed to classify that samples into islanding and non-islanding cases.

4.2 Power System Faults Simulation Results Analysis

4.2.1 Simulation Cases

To train the ANN classifier, different types of islanding and non-islanding cases have been tested listed in Table 4-1 including:

- Random switching of distribution line circuit breakers on both low and medium voltage distribution, this tripping occurs at wide range of active power flow, and can describe the general possible disturbance at the PCC.
- Organized circuit breaker tripping in particular cases that describes small margin of active power flow mismatch, hence, critical cases of NDZ can be tested, particularly when ΔP is below 20%.
- Load switching on and switching off along the distribution lines, and also load variation.
- Switching capacitor banks connected in two positions to the grid at different values of reactive power compensation.

Table 4-1: Events list simulation description under islanding and non-islanding operation

Event Type	Action	Description	Number
Islanding	Tripping circuit breakers (CB1, CB3, and CB7).	Tripping happens at different times along the voltage waveform (mainly at 0, 45, 90, and 135 degrees), at different active power flow mismatch and at different loading.	64
Phase to phase faults	Line-line short circuit at different locations/buses along the distribution system.	Faults happens at different times along the voltage waveform (mainly at 0, 45,90, and 135 degrees), at different power flow mismatch	21
Single phase to ground fault	Line-ground short circuit at different locations/buses before the PCC at the grid side.		10
Three phase faults	Three phase faults, and three phase-ground bolted short circuit at distribution buses before the PCC at the grid side.		22
Load switching and load changing	Switching on or off load 1 and load 2.	Switching on and switching off circuit breakers CB4 and CB6 to connect or disconnect the load totally, and varying the load powers to simulate the operation of normal power changing.	11
Capacitor switching	Switching on or off capacitive power compensators 1, and 2.	Switching on and switching off circuit breakers CB2 and CB9 to raise or lower the capacitive power in the distribution system.	12

Figure 4-1 shows MATLAB/ SIMULINK schematic diagram of the power distribution-inverter interconnected system corresponding to the studied system in Figure 3-1. Furthermore, Figure 4-2 shows all measurement tools, mathematical operations, data processing, and data transfer blocks used in simulation process.

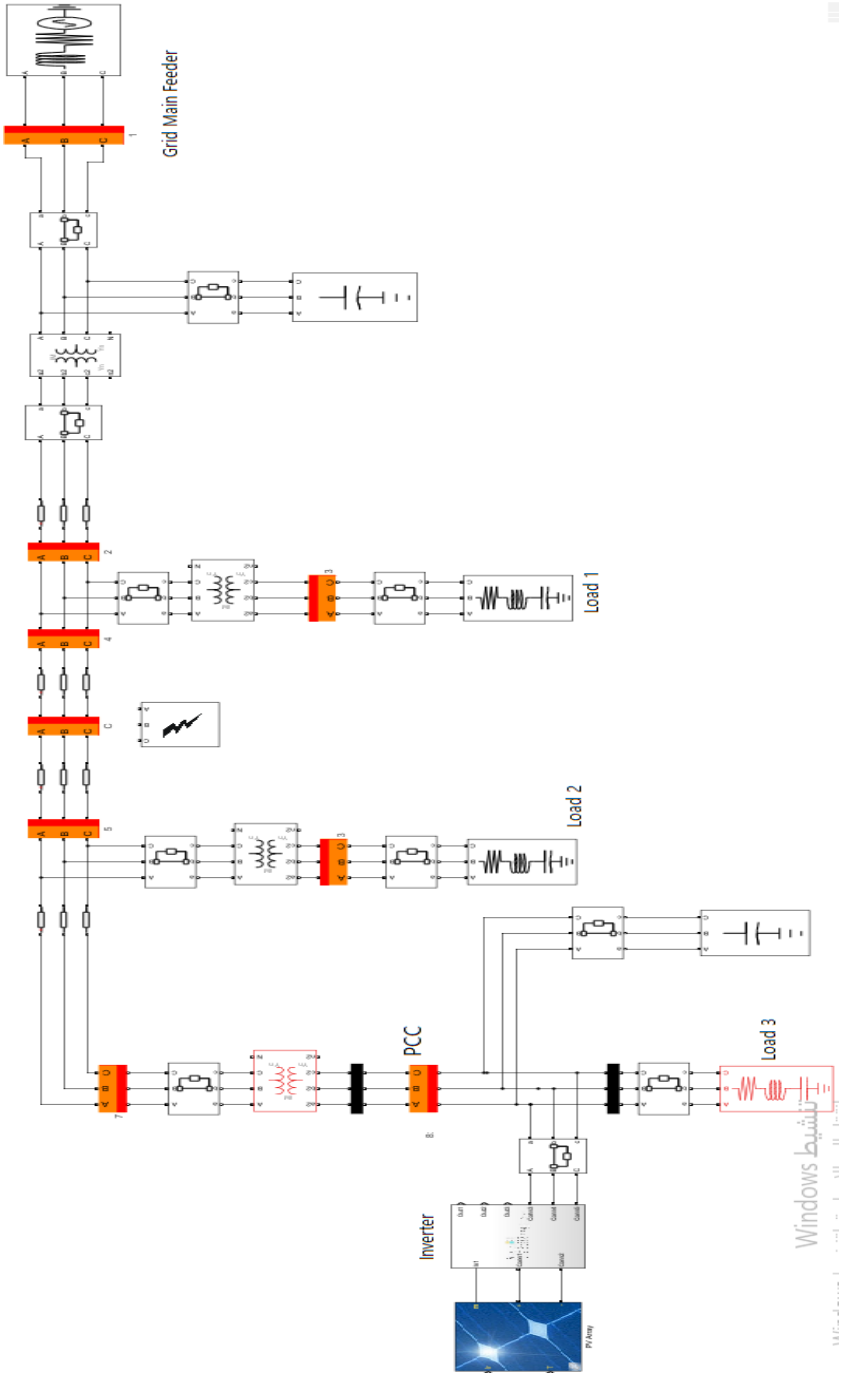

Figure 4-1: SIMULINK diagram of the power distribution system

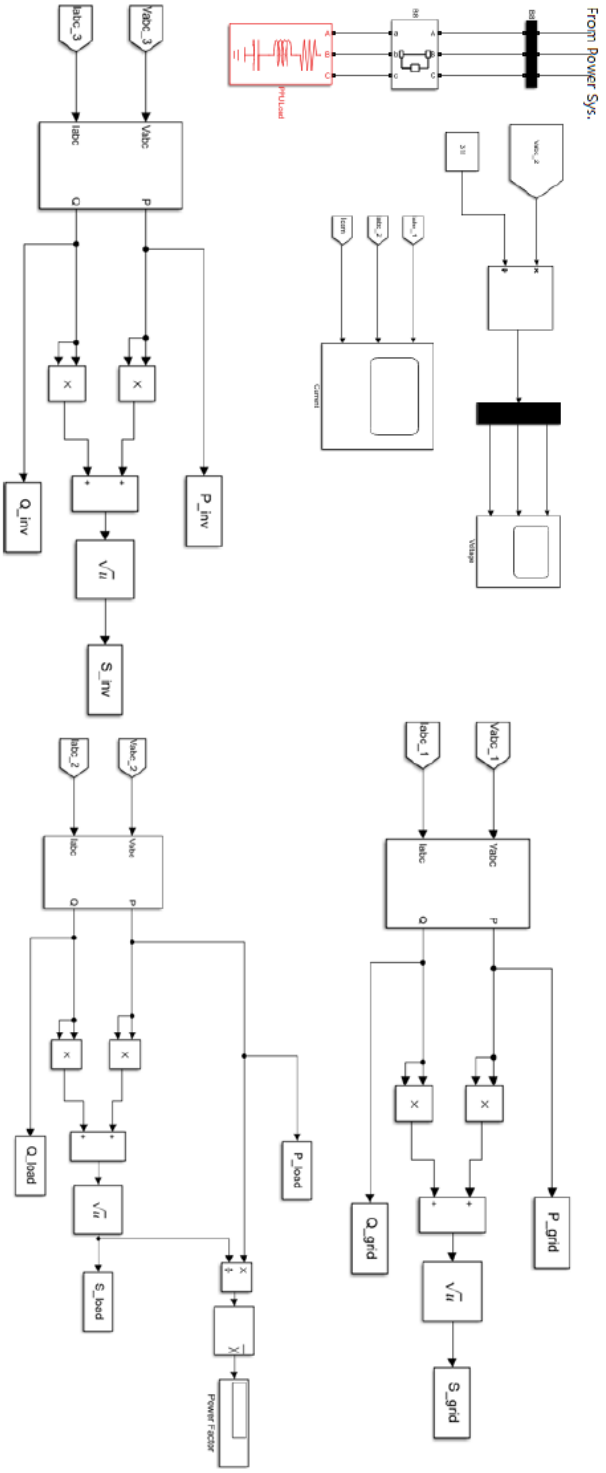

Figure 4-2: SIMULINK diagram for measurements

4.2.2 Waveform Simulation Time Frame

Simulation time frame covers 12 voltage cycles, divided into:

- First 5 voltage cycles: dedicated for grid-inverter initialization where the voltage and current waveforms are not stable yet. Hence, no events are tested during this time, see (Window 1) in Figure 4-3.
- From the 6th to the 10th voltage cycles: all events are tested during this time, see (window 2) in Figure 4-3. These 5 cycles represent 0.1 second; very short time period compared to IEEE standards for islanding detection time [6].
- Cycles 11, and 12 are added to complete the 5 cycles when the event location is shifted from the beginning (in cycle number 6).

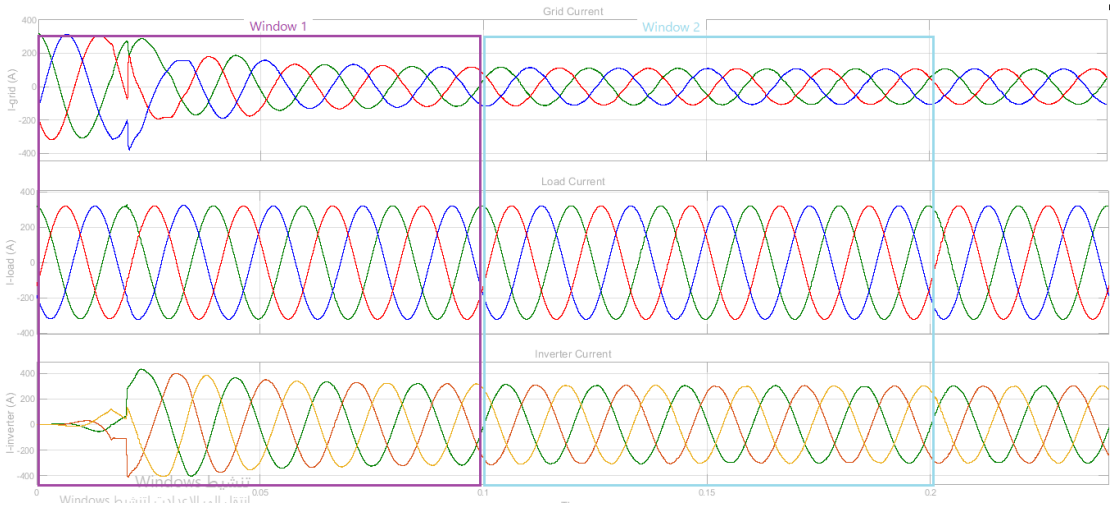

Figure 4-3: Three phase current waveforms; simulation time frame windows

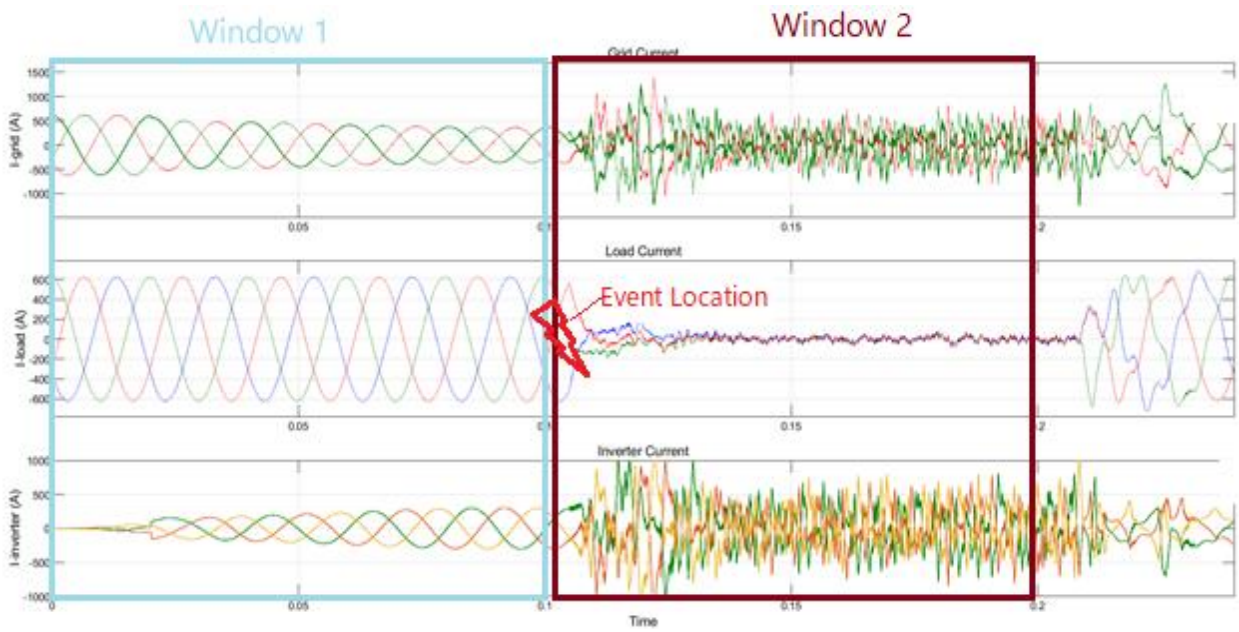

Figure 4-4: General 3 phase fault; current waveforms

4.3 Events Simulation

The following five cases are introduced in this chapter for discussion and analysis, they include 2 islanding cases and 3 non-islanding cases with conditions listed in Table 4-2, each with its corresponding ΔP, and the absolute value of ΔP is taken below 10% to test the worst case of the NDZ. All measurements are depending on choosing 'd4' as the mother wavelet of DWT.

Table 4-2: Energy content of detail coefficients for the 5 analyzed cases

Case No.	Event Type	Location	Abs (ΔP)	Energy Content Coefficients of the 5 Levels of DWT				
				D_1	**D_2**	**D_3**	**D_4**	**D_5**
1	Islanding (Event 116)	Tripping (CB7)	4.62%	111.74	111.48	110.72	63.60	39.75
2	Three phase short circuit (Event 118)	At load bus, after T4, on the PCC	5.22%	8.61	13.64	13.42	8.81	15.49
3	Capacitor switching (Event 119)	Capacitor 1 (CB2)	5.22%	3.19	4.07	5.44	10.33	19.97

4	Islanding (Event 129)	Tripping (CB7)	1.47%	6.99	8.23	13.54	24.89	43.73
5	Load switching (Event 131)	Load 1(CB4)	1.47%	1.56	2.57	5.11	10.13	19.96

An islanding event, case 1 represents event number 116 in Table 4-3 has been simulated by tripping circuit breaker CB7 to disconnect the load transformer, the absolute value of ΔP is about 4.6%, the detail coefficients are clearly larger than case 4 which was recorded in smaller ΔP (1.47%). The variations in voltage waveforms during islanding time period between case 1 and case 4 noticed in Figure 4-5 and Figure 4-6 explain the differences between the details coefficients shown. On the other hand, among non-islanding events, three phase short circuit represented by case 2 has the largest energy content in its details as clearly illustrated in Figure 4-9, Figure 4-9, Figure 4-11, Figure 4-9, and Figure 4-9 which show the voltage and current waveforms for each case.

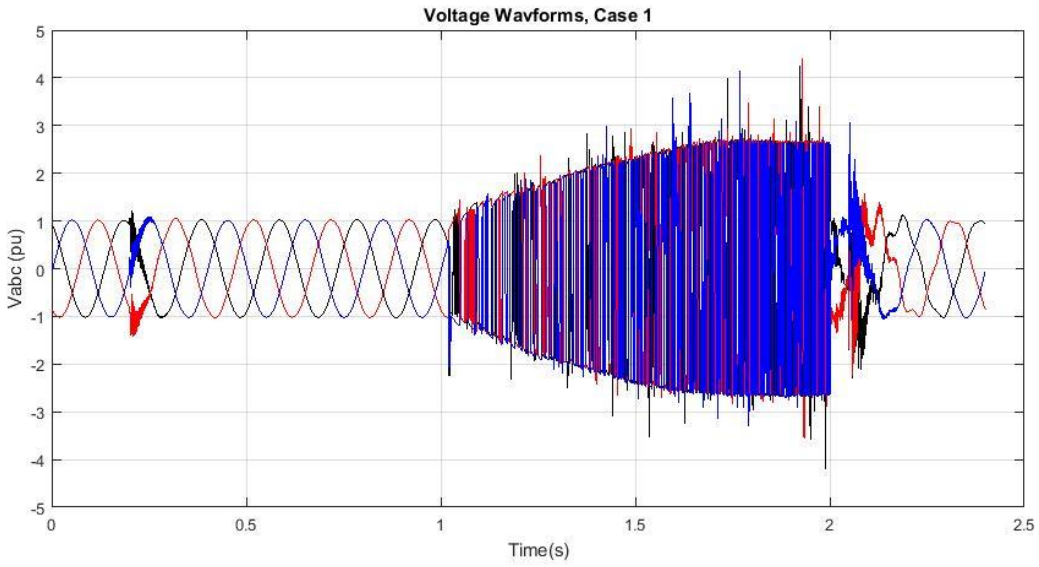

Figure 4-5: Voltage waveform at the PCC, case 1

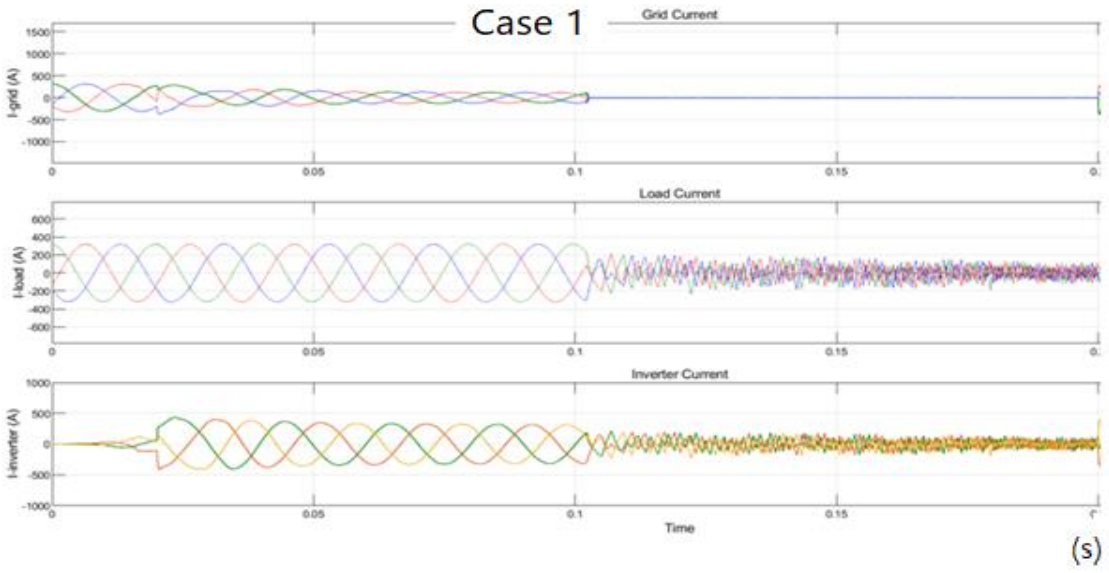

Figure 4-6: Current waveform at the PCC, case 1

The DWT decomposition has been simulated using MATLAB applications toolbox. Figure 4-9, Figure 4-9, Figure 4-11, Figure 4-9, and Figure 4-9 show the wide variations between the DWT details coefficients for each case during the 5 cycles time period of the event duration.

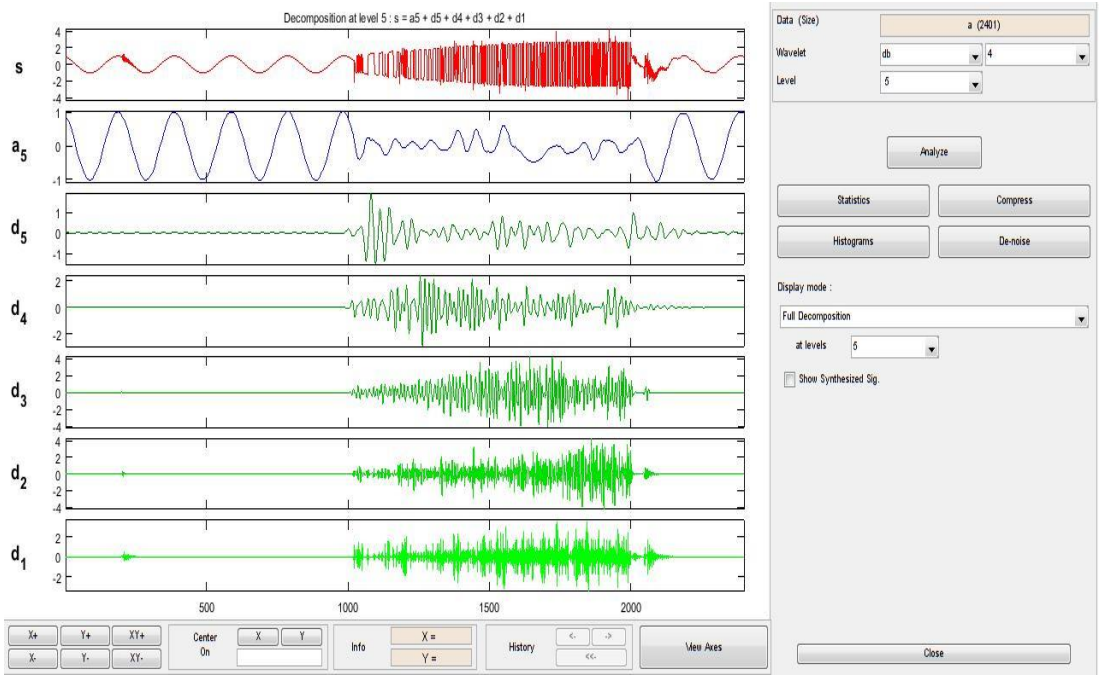

Figure 4-7: Details coefficients of DWT decomposition, case 1

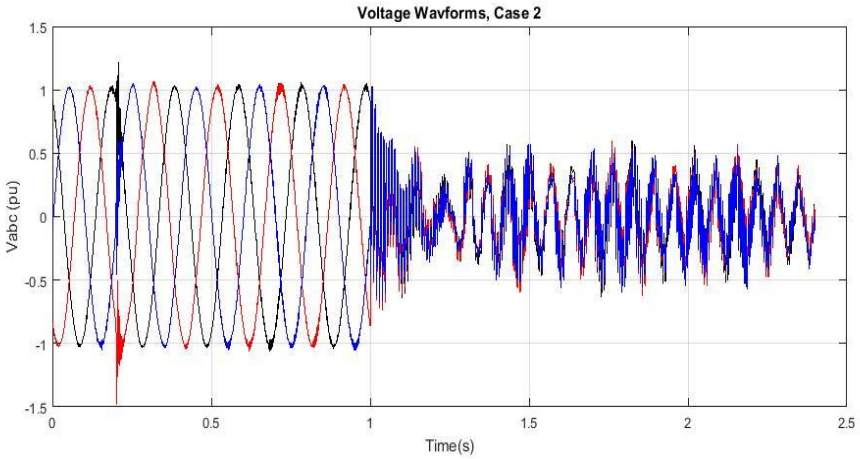

Figure 4-8: Voltage waveform at the PCC, case 2

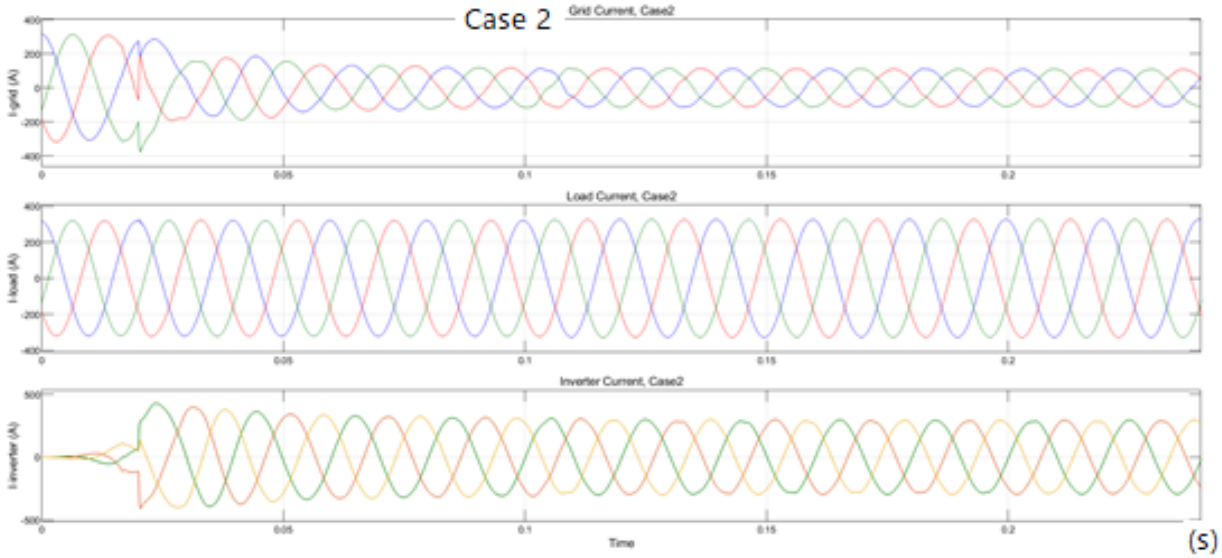

Figure 4-9: Current waveform at the PCC, case 2

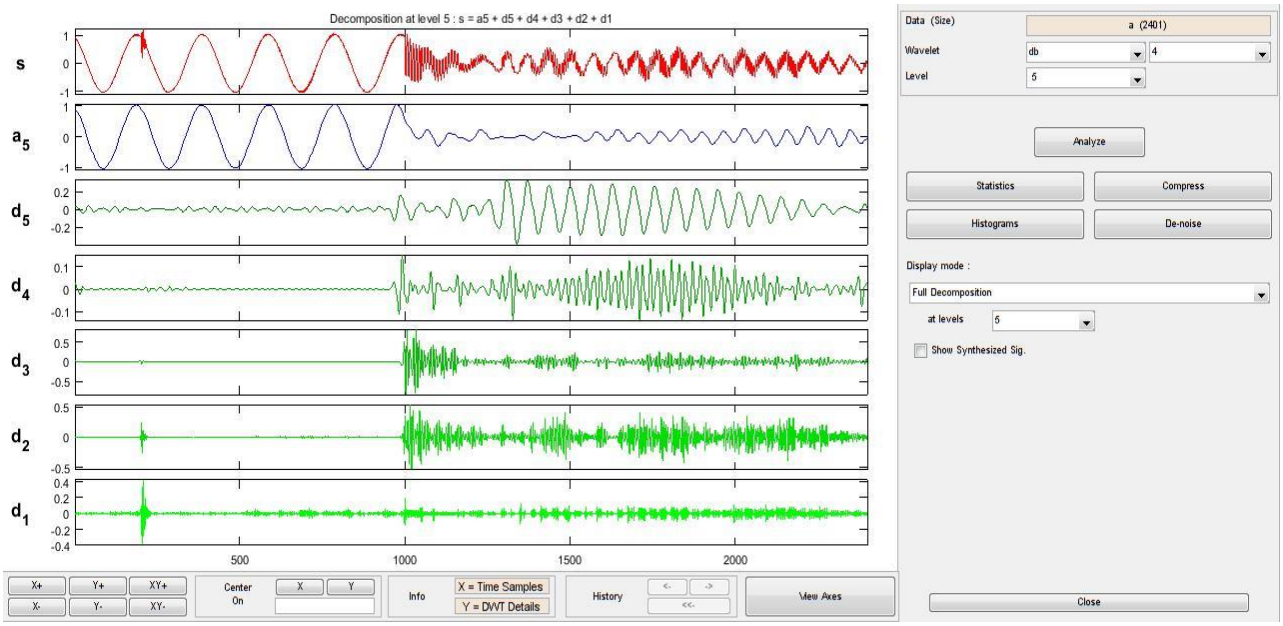

Figure 4-10: Details coefficients of DWT decomposition, case 2

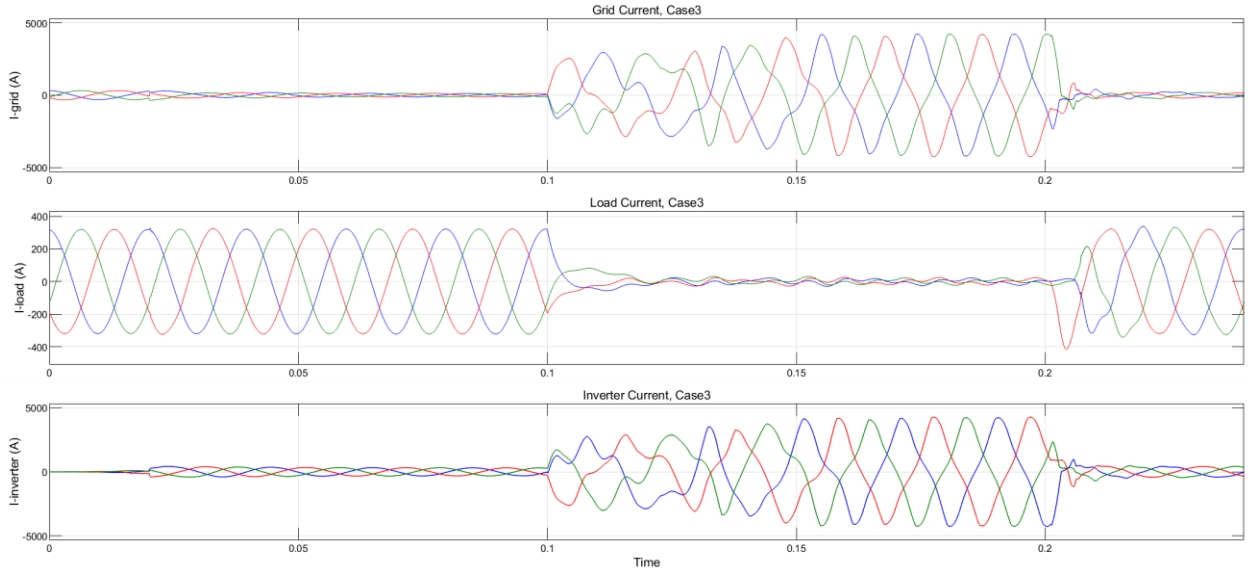

Figure 4-11: Current waveform at the PCC, case 3

In cases 3 and 5, there is very low detail coefficients compared to islanding and fault cases, this seems to be discriminative factor that can be utilized to distinguish between islanding details pattern and the disturbances caused by such load and capacitor switching. On the other hand, some islanding events recorded have showed such smaller details very close numerically to load

switching details, therefore, an intelligent method is required to classify these events, hence adopting the ANN classifies in this study is strongly justified.

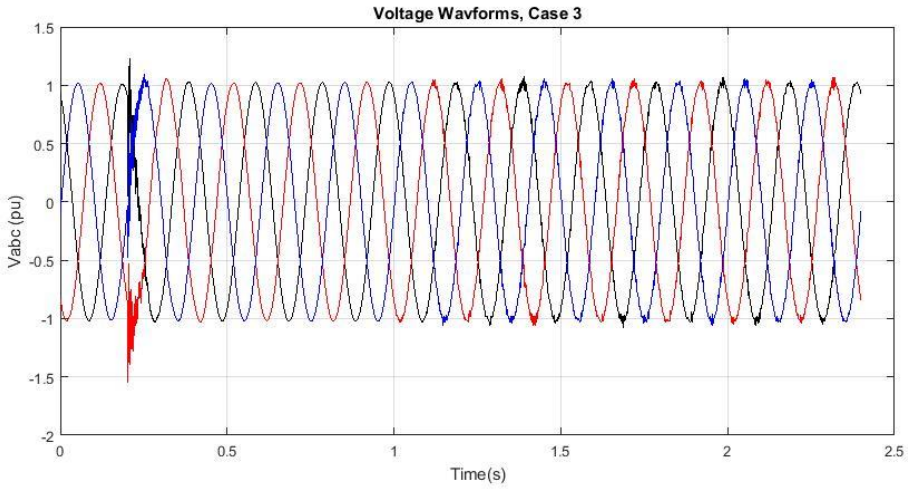

Figure 4-12: Voltage waveform at the PCC, case 3

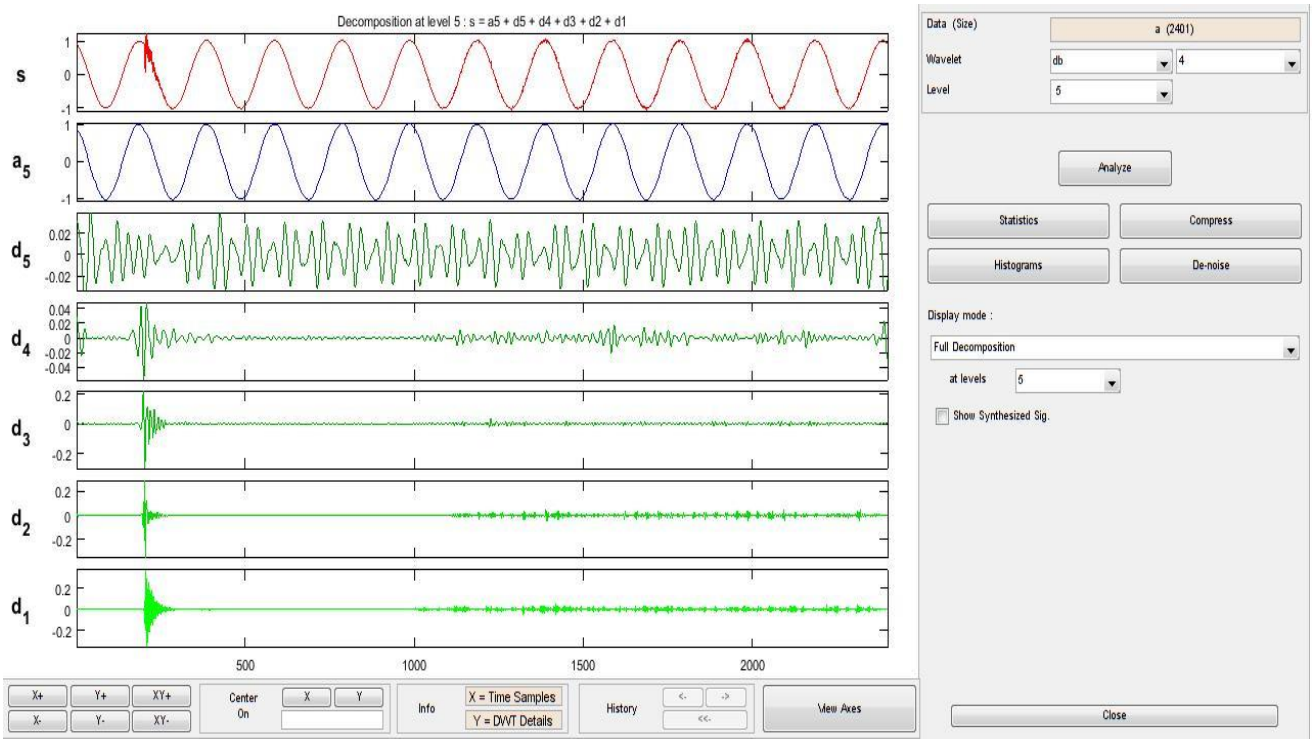

Figure 4-13: Details coefficients of DWT decomposition, case 3

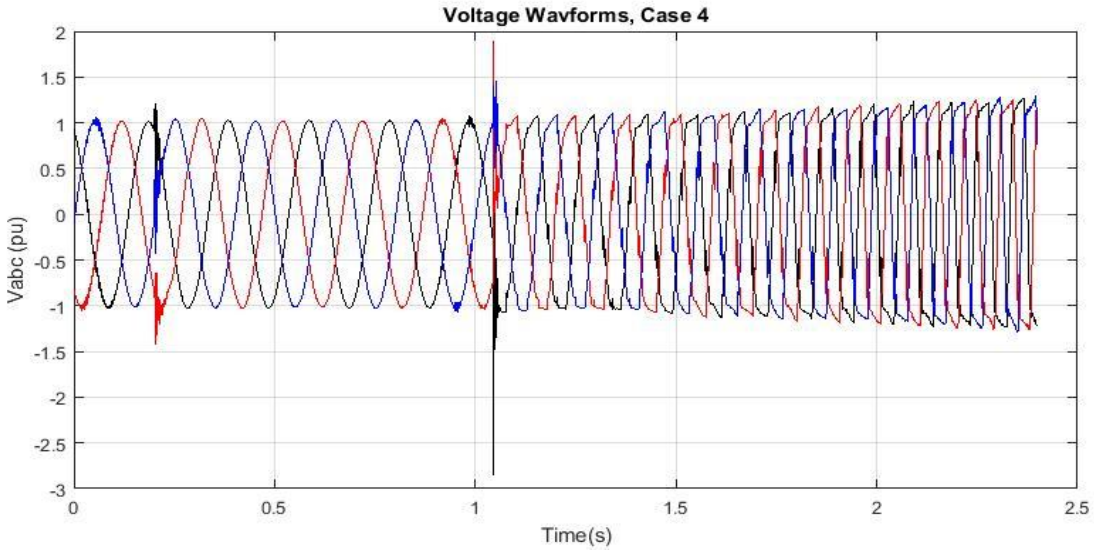

Figure 4-14: Voltage waveform at the PCC, case 4

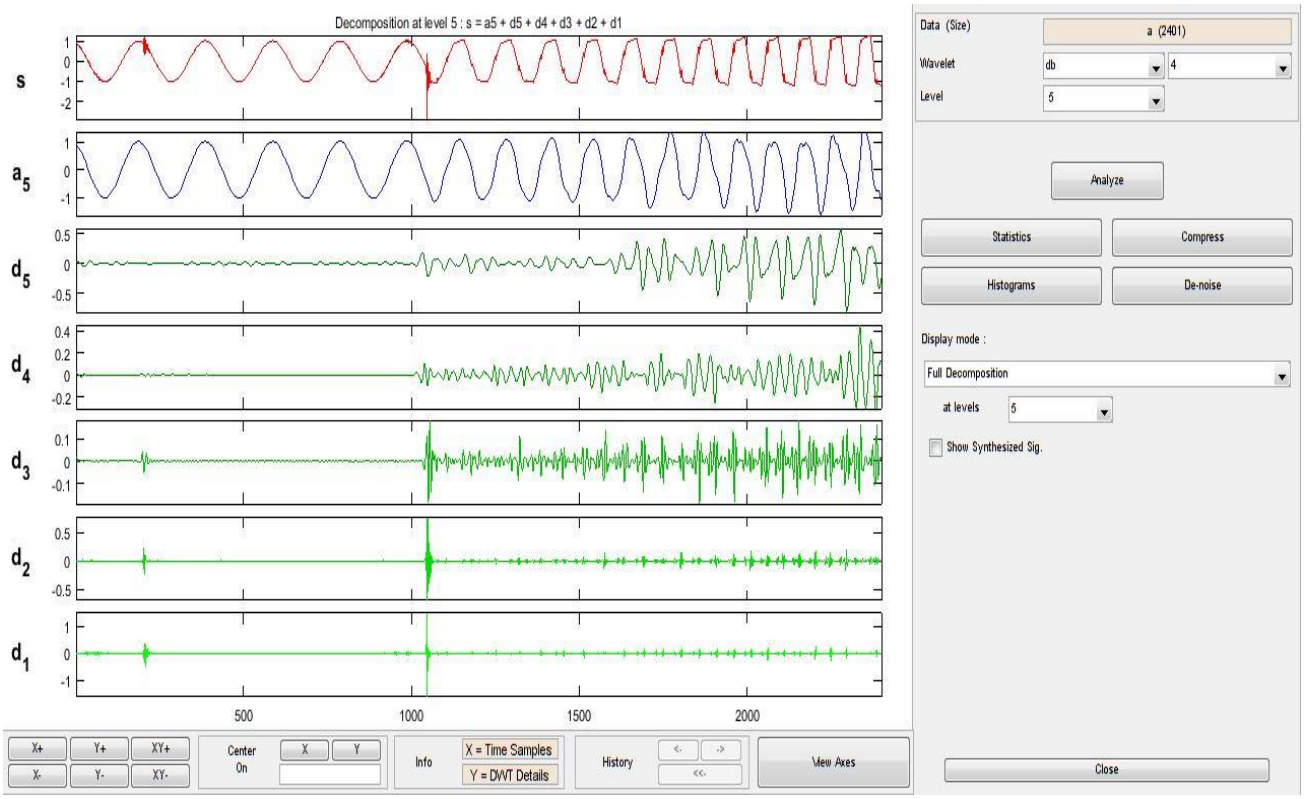

Figure 4-15: Details coefficients of DWT decomposition, case 4

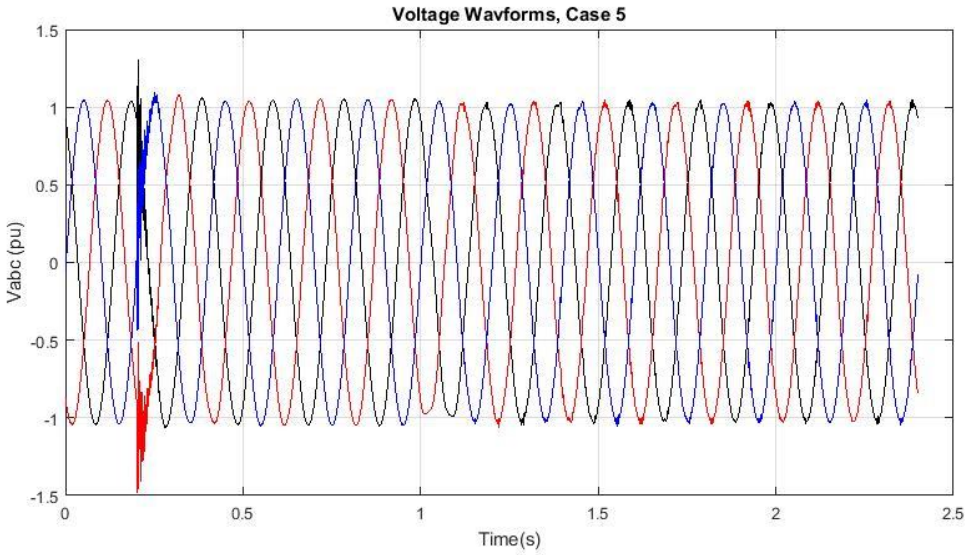

Figure 4-16: Voltage waveform at the PCC, case *5*

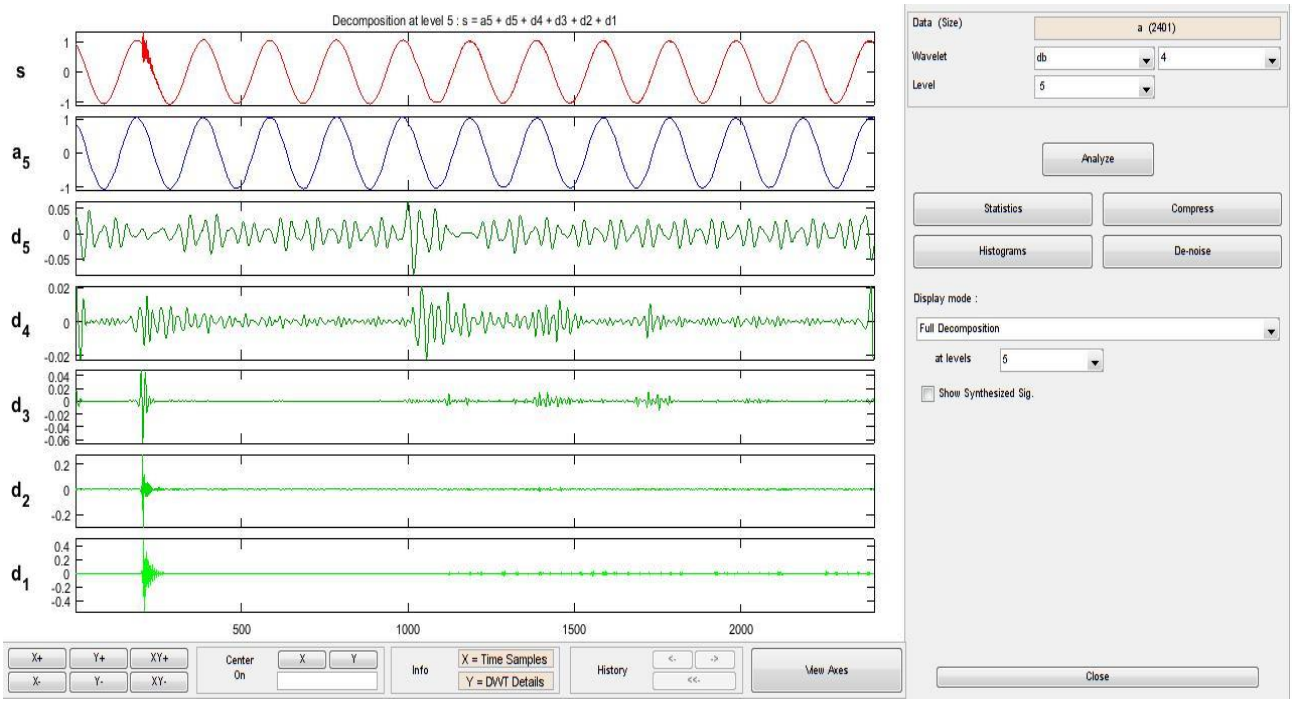

Figure 4-17: Details coefficients of DWT decomposition, case 5

4.4 ANN Training Analysis

4.4.1 ANN Training Overview

The 140 tested events listed in Table 4-3 with their corresponding 5- level DWT energy density-based detail coefficients are introduced as one input matrix to the feed forward back propagation artificial neural network classifier programed using MATLAB m-file editor. The output fed to the trained ANN is a single output where indicator (1) refers to islanding events, and indicator (0) refers to non-islanding events.

Table 4-3: The 140 tested events list, and their corresponding DWT energy density details

No.	Event	Location	Event Angle	Abs (ΔP)	Event Output Indicator	DWT Energy Density Coefficients				
						D_1	D_2	D_3	D_4	D_5
1	A-G Fault	Bus 1	0	68.9	0	0.046	0.3	0.74	0.91	2.7
2	B-G Fault	Bus 1	0	53.3	0	0.489	1.88	3.1	1.46	3.54
3	C-G Fault	Bus 1	0	61.3	0	0.517	1.84	4.47	1.94	3.42
4	A-B Fault	Bus 1	0	61.3	0	0.468	2.96	7.85	8.56	14.8
5	A-B-C Fault	Bus 1	0	61.3	0	0.583	3.71	8.62	8.72	13.9
6	A-B-C Fault	Bus 1	45	61.3	0	109.3	61.9	64.6	60.5	31.7
7	A-B-C-G Fault	Bus 1	45	56.4	0	106.2	63.9	71.8	67.2	41.3
8	A-B-C-G Fault	Bus 1	90	61.8	0	97.97	65.9	73.7	64.7	37
9	A-B-C-G Fault	Bus 1	90	392	0	68.97	41.5	48.6	45.8	25.7
10	A-B-C-G Fault	Bus 1	135	179	0	96.44	62.4	56.9	60.4	33.3
11	A-B-C-G Fault	Bus 1	0	86.6	0	89.54	63.7	70.6	53.8	32.3
12	A-B-C-G Fault	Bus 1	90	86.6	0	95.9	61.6	65.8	58.1	31.2
13	Islanding	Bus 1-CB 1	90	101	1	1.696	0.37	0.51	0.63	2.47
14	Islanding	Bus 1-CB 1	90	5.8	1	0.007	0.11	0.41	0.51	1.91
15	Islanding	Bus 1-CB 1	90	18.8	1	0.007	0.12	0.4	0.51	1.95
16	Islanding	Bus 1-CB 1	90	383	1	0.006	0.11	0.4	0.5	1.79
17	Islanding	Bus 8-CB 8	90	17.3	1	8.787	8.03	6.43	7.77	15.1

18	Islanding	Bus 8-CB 8	180	70.6	1	11.81	8.09	14.1	15.1	15.5
19	Islanding	Bus 8-.B 8	45	156	1	30.8	20.7	19.6	22.9	13.9
20	Islanding	Bus 8-CB 8	180	146	1	11.81	8.09	14.1	15.1	15.5
21	Islanding	Bus 8-CB 8	90	134	1	333.6	111	26	29.4	15.2
22	Islanding	Bus 8-CB 7	90	26.6	1	234.8	45.6	20.2	2.94	7.55
23	Islanding	CB3	90	192	1	28.77	15.6	10.5	6.28	10.2
24	Islanding	CB3	90	21.6	1	65.31	27.1	18.3	10.9	12.7
25	Islanding	CB3	90	45.5	1	58.19	30.2	17.5	9	11.4
26	Islanding	CB3	90	9.3	1	50.1	23.2	16.6	12.7	12.8
27	Islanding	CB3	90	228	1	40.83	19.3	15.8	9.76	11.9
28	Islanding	CB3	0	228	1	69.68	23.9	13.7	9.62	11.7
29	Switching Off Load1	CB4	0	47	0	1.785	0.55	0.63	0.84	2.6
30	Switching OnLoad1	CB4	0	48.9	0	2.018	0.67	0.68	1.15	2.79
31	Load 1 On: 400Kw	CB4	0	5.67	0	1.086	0.55	0.66	0.97	2.64
32	Switching Off Loads 1 & 2 (400,291)	CB4, CB6	0	33.8	0	0.014	0.17	0.49	1.01	4.19
33	Switching On Loads 1 & 2	CB4, CB6	0	33.8	0	0.011	0.15	0.47	0.91	3.08
34	Off Load 2	CB6	0	33.8	0	0.011	0.15	0.45	0.76	2.84
35	Switching Off Loads 1 & 2 (1000,291)	CB4, CB6	0	13.5	0	0.009	0.13	0.42	0.62	2.61
36	Switching On Loads 1 & 2 (1000,291)	CB4, CB6	0	13.5	0	0.012	0.16	0.49	0.9	3.34
37	A-G Fault	Bus 8	0	221	0	0.044	0.34	0.87	3	6.56
38	B-G Fault	Bus 8	0	221	0	0.203	1.46	3.65	4.64	7.47
39	C-G Fault	Bus 8	0	221	0	0.229	1.62	3.26	5.41	6.86
40	A-B Fault	Bus 8	180	221	0	0.233	0.64	1.6	4.87	9.02
41	B-C Fault	Bus 8	90	221	0	0.083	0.52	1.47	5.08	9.09
42	A-C Fault	Bus 8	180	221	0	0.298	0.63	1.71	4.91	8.53

43	A-B-C Fault	Bus 8	90	221	0	0.56	1.42	1.05	2.58	4.37
44	A-B-C-G Fault	Bus 8	90	221	0	0.559	1.4	0.78	1.53	4.14
45	A-G Fault	Bus 8	90	38.6	0	0.354	1.41	3.47	5.34	8.99
46	B-G Fault	Bus 8	45	38.6	0	0.589	1.14	2.88	6.58	7.61
47	C-G Fault	Bus 8	0	38.6	0	0.228	1.61	3.28	5.53	7.27
48	A-B Fault	Bus 8	180	38.6	0	0.138	0.9	2.61	6.64	13.8
49	B-C Fault	Bus 8	0	38.6	0	0.257	1.14	2.58	7.88	14.9
50	A-C Fault	Bus 8	0	38.6	0	0.219	1.4	2.73	7.26	14.2
51	A-B-C Fault	Bus 8	180	38.6	0	0.512	0.87	2.08	6.51	18.9
52	A-B-C-G Fault	Bus 8	0	38.6	0	0.342	2	2.25	6.1	18.9
53	A-G Fault	Bus 8	45	6.01	0	0.416	0.85	2.51	5.32	7.73
54	B-G Fault	Bus 8	45	6.01	0	0.576	1.11	2.87	6.51	8.01
55	C-G Fault	Bus 8	45	6.01	0	0.216	0.49	1.39	3.84	7.77
56	A-B Fault	Bus 8	45	6.01	0	0.926	1.33	3.54	9.22	14.9
57	B-C Fault	Bus 8	45	6.01	0	0.73	1.13	3.35	8.33	14.7
58	A-C Fault	Bus 8	45	6.01	0	0.237	0.88	3.28	8.3	14.7
59	A-B-C Fault	Bus 8	45	6.01	0	1.049	1.04	2.83	10.3	17.3
60	A-B-C-G Fault	Bus 8	45	6.01	0	1.06	1	1.28	2.71	5.14
61	Cap0. On - 250 kVAR	CB2:At 33KV	0	18.8	0	5.209	7.45	2.92	2.98	5.91
62	Cap1. Off	CB2:At 33KV	0	18.8	0	2.009	0.93	0.72	1.1	2.56
63	Cap1. 250 to 130 kVAR	CB2:At 33KV	0	6.38	0	2.011	0.94	0.74	1.3	2.67
64	Cap1. 130 to 250 kVAR	CB2:At 33KV	0	6.38	0	3.511	4.29	1.67	1.83	3.9
65	Cap0 On	At C: At 11KV	90	21	0	6.661	4.68	1.93	3.67	7.1
66	Cap0 Off	At C: At 11KV	90	17.8	0	1.994	0.88	0.69	0.89	2.51
67	Cap0 130 to 250 kVAR	At C: At 11KV	90	20.1	0	2.228	1.11	0.78	1.28	2.79
68	Cap0 250 to 130 kVAR	At C: At 11KV	90	20.5	0	2.016	0.97	0.72	1.29	2.69
69	Cap2 On	CB11: At 0.4KV	90	21.7	0	27.41	19.6	13.9	10.7	6.89

70	Cap2 Off	CB11: At 0.4KV	90	19.4	0	2.098	0.92	0.76	1.27	2.69
71	Cap1 50 to 70 kVAR	CB11: At 0.4KV	90	22.7	0	1.998	0.96	0.7	1.28	2.7
72	Islanding	Tripping CB3	0	3.13	1	46.24	22.9	13.5	9.79	9.5
73	Islanding	Tripping CB3	45	3.13	1	45.16	24	13.1	11.3	12.3
74	Islanding	Tripping CB3	90	3.13	1	44.94	23.2	15.3	10.8	10.5
75	Islanding	Tripping CB3	135	3.13	1	42.74	21.8	16.4	12.2	14.2
76	Islanding	Tripping CB3	90	3.13	1	0.819	0.34	0.52	0.64	2.49
77	Islanding	Tripping CB3	45	3.13	1	0.404	0.23	0.41	0.54	2.15
78	Islanding	Tripping CB3	90	3.13	1	0.391	0.22	0.41	0.55	2.16
79	Islanding	Tripping CB3	0	3.13	1	0.387	0.23	0.42	0.58	2.26
80	Islanding	Tripping CB3	0	3.13	1	0.418	0.23	0.42	0.71	2.9
81	Islanding	Tripping CB7	0	3.13	1	4.194	4.04	4.41	10.4	25.6
82	Islanding	Tripping CB7	45	3.13	1	3.987	3.69	4.55	9.64	24.8
83	Islanding	Tripping CB7	45	2.68	1	0.012	0.16	0.51	1.27	5.13
84	Islanding	Tripping CB7	45	4	1	0.012	0.17	0.51	1.18	5.23
85	Islanding	Tripping CB7	45	0.35	1	0.011	0.16	0.46	1.01	5.06
86	Islanding	Tripping CB7	45	0.69	1	0.011	0.16	0.5	1.06	5.26
87	Islanding	Tripping CB7	45	1.41	1	0.011	0.16	0.5	1.09	5.25
88	Islanding	Tripping CB7	45	3.97	1	0.012	0.17	0.5	1.2	5.3
89	Islanding	Tripping CB7	45	4	1	0.012	0.17	0.51	1.18	5.23
90	Islanding	Tripping CB7	0	1.41	1	0.011	0.16	0.5	1.18	5.2
91	A-G Fault	At bus 2	90	0.7	0	0.434	2.84	6.64	3.3	10.4
92	B-G Fault	At bus 2	90	1.37	0	0.263	1.85	4.32	2.08	9
93	C-G Fault	At bus 2	90	1.37	0	0.198	1.37	2.66	2.55	7.67
94	A-B Fault	At bus 2	90	1.37	0	0.623	3.07	7.47	5.93	12.7
95	A-C Fault	At bus 2	90	1.37	0	0.656	3.85	9.68	6.33	11.9
96	B-C Fault	At bus 2	45	1.37	0	0.819	3.88	9.7	6.56	8.72

97	A-B-C	At bus 2	90	1.37	0	0.134	1.12	3.28	4.8	10.7
98	A-B-C-G Fault	At bus 2	90	1.37	0	1.753	15.3	40.5	15	15.8
99	Islanding	Tripping CB3	0	1.37	1	0.008	0.12	0.41	0.62	2.25
100	Islanding	Tripping CB3	90	1.37	1	0.007	0.11	0.41	0.61	2.45
101	Islanding	Tripping CB3	90	88.5	1	0.008	0.12	0.39	0.65	2.34
102	Islanding	Tripping CB3	90	83	1	0.007	0.11	0.41	0.67	2.18
103	Islanding	Tripping CB3	135	577	1	0.009	0.12	0.4	0.92	3.17
104	Islanding	Tripping CB3	45	577	1	0.009	0.12	0.4	0.93	3.18
105	Islanding	Tripping CB3	90	577	1	0.009	0.12	0.4	0.92	3.17
106	Islanding	Tripping CB3	45	577	1	3.947	1.56	2.03	3.3	14.9
107	Islanding	Tripping CB3	45	577	1	3.229	1.73	2.28	3.71	16.5
108	A-B-C Fault at C	C	90	577	0	53.88	32.2	34.2	34.8	25.7
109	A-B-C Fault at C	C	0	16.9	0	59.68	50	44.2	19.1	11.2
110	Islanding	Tripping CB1	0	16.9	0	33.04	30.1	22.2	10.8	16.1
111	A-B-C Fault	Bus 1	0	16.9	0	91.37	71.9	52.4	29.1	30.1
112	A-B-C Fault	Bus 1	0	14.3	0	116.8	67.4	64.1	30.8	23.2
113	Islanding	Tripping CB1	0	14.3	1	46.82	32.5	30.5	14.5	20.4
114	Fault	Bus 8	0	14.3	0	11.62	19.5	13	8.74	21
115	Islanding	Tripping CB3	0	14.3	1	92.73	95.2	136	79.1	37.4
116	Islanding	Tripping CB3	0	4.61	1	87.58	114	124	75.2	34.3
117	A-B	Bus 8	0	5.23	0	23.66	8.84	11.6	12.5	16
118	A-B-C Fault	Bus 8	0	5.23	0	3.896	14.8	13.4	4.4	18.5
119	C1 Switching ON	CB2	0	5.23	0	2.008	3.86	2.52	1.91	3.22
120	C2 Switching Off 30%	CB9	0	5.23	0	1.312	1.24	0.73	0.75	2.52
121	Switching Off Load 2	CB6	0	5.23	0	2.251	0.69	0.72	1.04	2.67
122	A-B-C-G Fault	Bus 8	0	5.23	0	10.09	4.68	3.55	3.45	7.82
123	A-B Fault	Bus 8	0	5.23	0	15.29	9.1	8.86	9.07	11.2

124	Islanding	Tripping CB3	0	5.23	1	48	20.2	13.3	9.12	9.18
125	Islanding	Tripping CB3	90	1.47	1	45.01	20.7	14.3	7.77	9.33
126	Islanding	Tripping CB3	90	1.47	1	38.13	22	13.5	10.1	9.94
127	Islanding	Tripping CB3	45	1.47	1	38.17	20.4	13.7	8.83	7.94
128	Islanding	Tripping CB3	135	1.47	1	38.74	19.2	13.3	9.16	8.4
129	Islanding	CB7: Load bus	45	1.47	1	5.588	5.39	5.3	12.8	25
130	Islanding	CB7: Load bus	90	1.47	1	4.427	5.49	5.91	12.6	24.2
131	Load 1 On: 400Kw	CB4	0	1.47	0	0.92	0.34	0.5	0.72	2.59
132	Load 2 OFF: 291Kw	CB6	45	1.47	0	2.298	0.68	0.69	0.96	2.63
133	Islanding	CB3	0	1.47	1	45.95	20.7	14.6	9.01	9.56
134	Islanding	CB3	45	1.47	1	38.06	16.6	12.7	7.73	9.41
135	Islanding	CB3	90	1.47	1	45.01	20.7	14.3	7.77	9.33
136	Islanding	CB7: Load bus	135	3.13	1	0.4	0.22	0.42	0.68	2.82
137	Islanding	CB3	135	3.95	1	24.63	13.8	11.2	8.51	7.63
138	Islanding	CB7: Load bus	0	3.95	1	2.438	3.58	5.67	15.9	31.2
139	Islanding	CB7: Load bus	45	5.35	1	2.856	3.56	5.18	12.6	27.6
140	Islanding	CB3	45	5.35	1	0.401	0.22	0.42	0.63	2.55

4.4.2 ANN Training Simulation

The neural network classifier shown in Figure 4-18 receives the 5 inputs, and arranged as 1-input matrix representing the 5-energy details ($D_1 - D_5$) of each event sample, 1 hidden layer with 100 neurons, and one output layer.

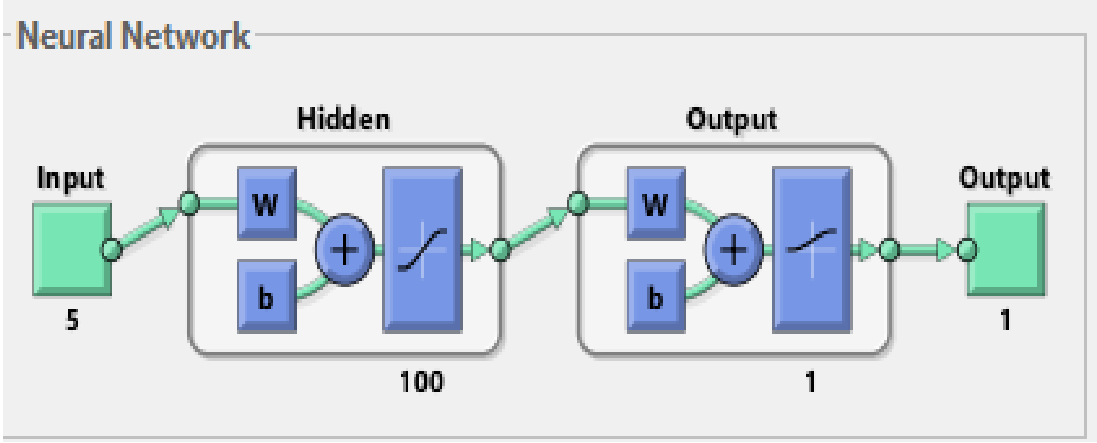

Figure 4-18: MATLAB schematic of the trained FFBP ANN

The 140 input samples are divided as follows:

- 70 %: for training, which equals 98 samples.
- 15%: for validation, which equals 21 samples.
- 15% for testing, which equals 21 samples.

- **Training Case 1: 40 Neurons Network**

After 32 iteration, the validation is 95.2%, and the total regression accuracy of the training is 92.1% as shown in regression matrices displayed on Figure 4-19.

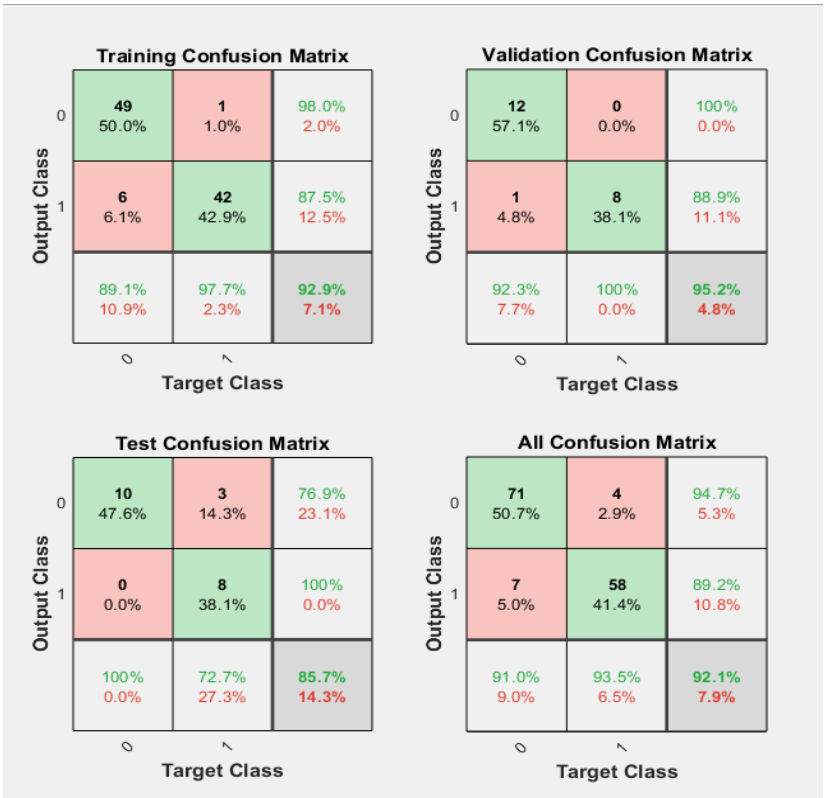

Figure 4-19: ANN regression results with number of neurons n=40

Performance of the training shown in Figure 4-20 illustrates that the best validation performance is 0.197, and the best training of this case lays on epoch 26 of training history.

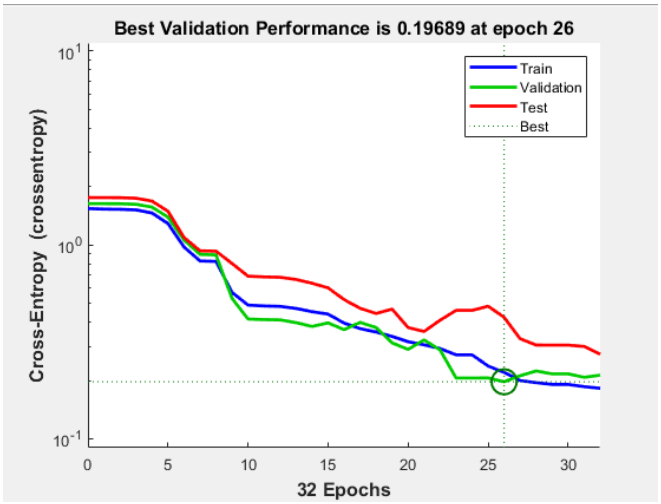

Figure 4-20: Performance of ANN training, n=40 neurons

- **Training Case 2: Comparison between 500 and 600 Neurons Networks**

Changing the neurons to 600 has raised the iterations to 41, and consequently improved the training regression to 98.6% according the confusion matrix shown in Figure 4-21. The best validation performance is reduced to 0.0305, as shown in Figure 4-22.

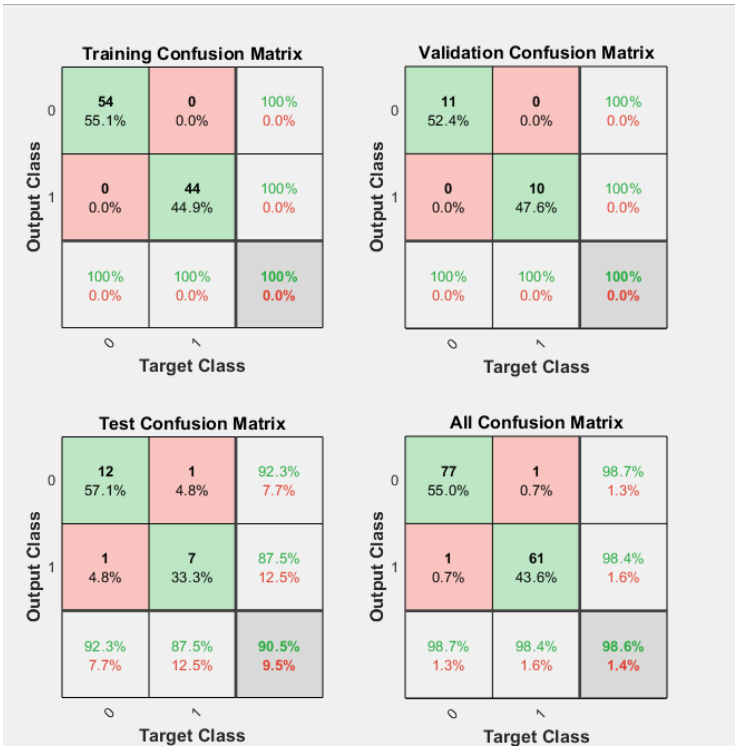

Figure 4-21: ANN regression results, neurons n=600

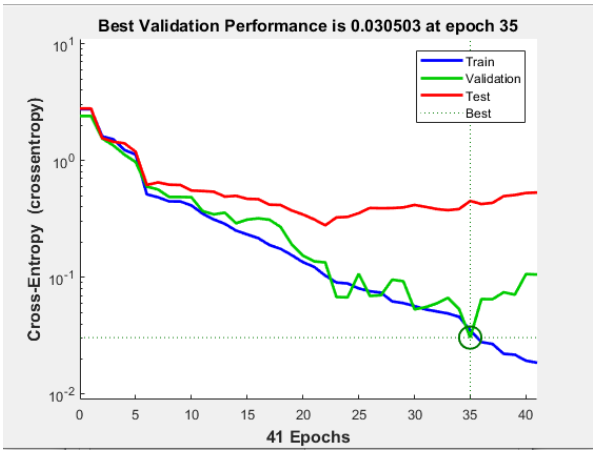

Figure 4-22: Performance of ANN training, n=600 neurons

4.4.3 Multilayer ANN Training

Changing the number of the hidden layers of the ANN sometimes applied to enhance the training results, hence as a result, the network complexity increases and the training time increases also. By using two hidden layers in the ANN applied in this study which schematic is shown in Figure 4-23, the training performance gets worse, where the average accuracy still below 90% and varies according to the chosen neurons value in each case.

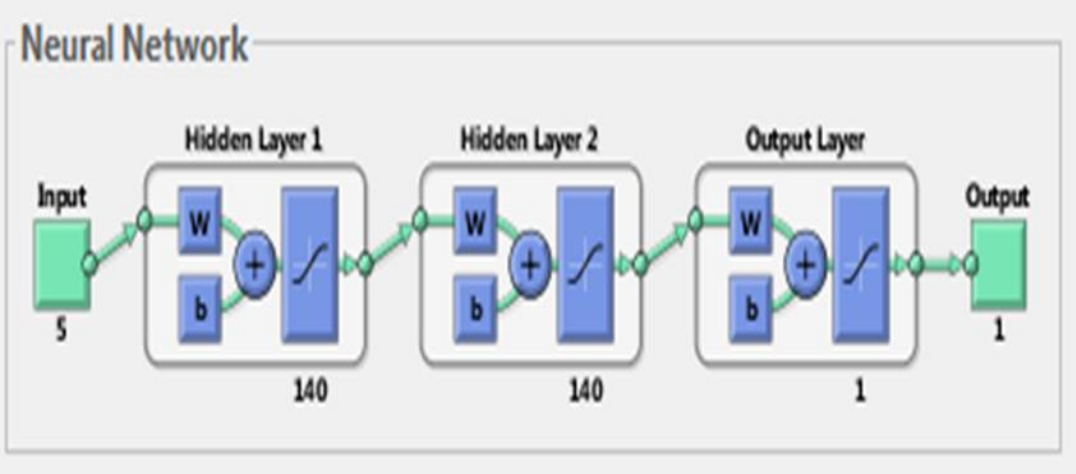

Figure 4-23: MATLAB schematic of the 2 hidden layers ANN

At 40 neurons, the average training regression is 89.3% as shown in Figure 4-24, and with very little improvement in training results; which is 90% in average at 600 neurons, as shown in Figure 4-25.

Figure 4-24: ANN Training regression for 2 hidden layers network, neurons=40

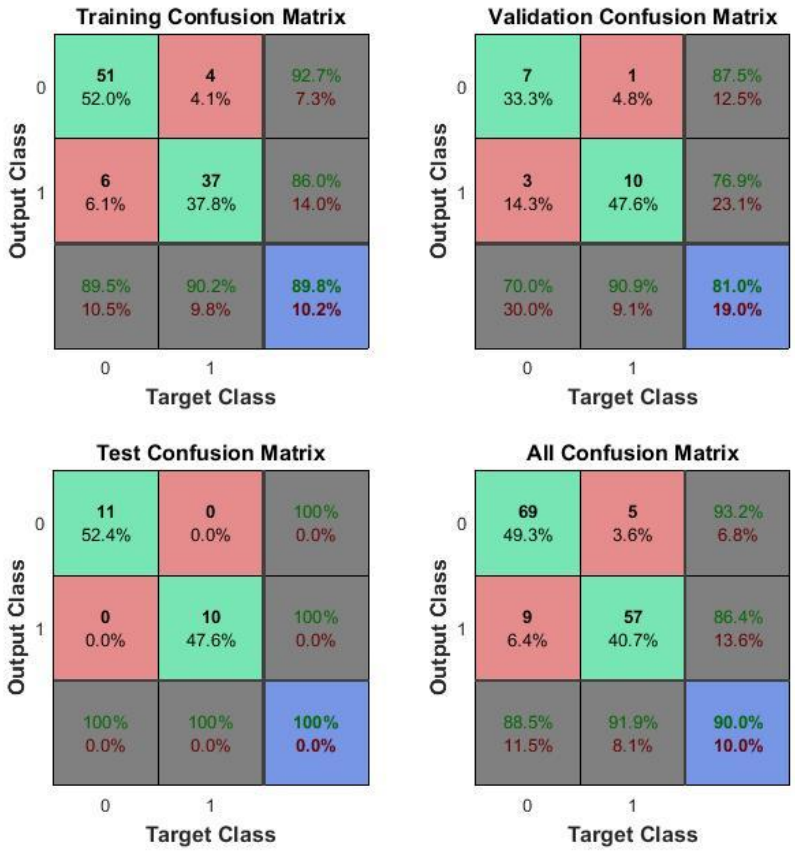

Figure 4-25: ANN Training regression for 2 hidden layers network, neurons=600

4.4.4 ANN Training at Low Power Mismatch

Referring to Table 4-3, and considering the events (53-100) and (109-140) when the power mismatch is below 20%, the training produced valuable results as seen in Figure 4-26, 97.5% accuracy is too close to whole events training accuracy with similar ANN parameters.

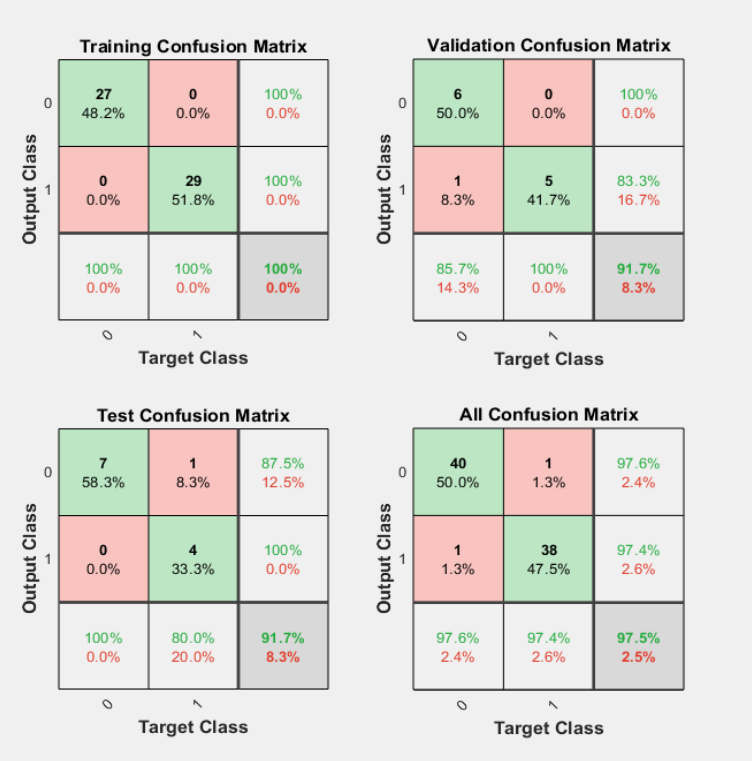

Figure 4-26: ANN Training regression at low power mismatch

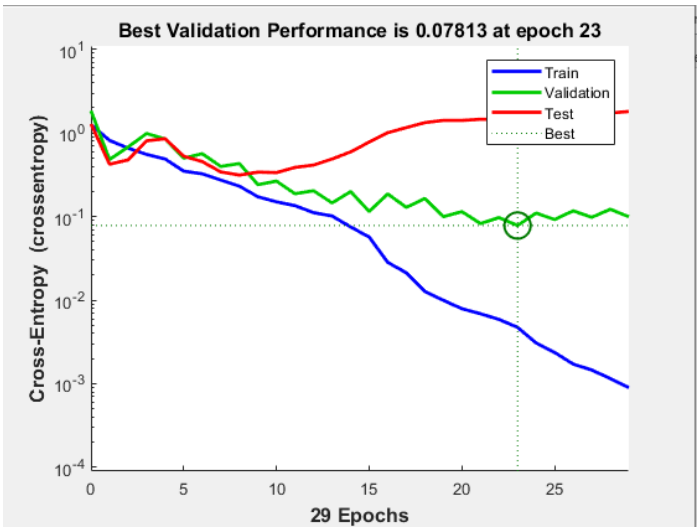

Figure 4-27: Performance of ANN training at low power mismatch

CHAPTER 5

5 Conclusions, Recommendations, and Future Work

5.1 Summary

In this study, real section of electrical distribution grid connected to PV DG inverter is tested to recognize its response against abnormal and abrupt system events. Intelligent approach including DWT based ANN islanding detection techniques is applied, and 140 different cases have been simulated using MATLAB/SIMULINK and m-file editor. Results generated the feature characteristic which describes the interconnected power system response to such events. Consequently, the ANN pattern classifier produced high accuracy detection, and within the islanding regulations according to IEEE 1547 standards.

5.2 Conclusions

According to the conducted study, and the simulation results, the following conclusions can be stated:

- The obtained results present an average accuracy of 90% – 98% in islanding detection according the simulation done for different training parameters.
- Appling the intelligent methods; like ANN with DWT on real grid-DG system is efficient technique in islanding detection. On the other hand, it is important to realize that the training is dependent of many factors, not only the input matrix pattern, but also the number of neurons and hidden layers, and activation function selected. Hence, the complexity would vary, and the training time as well.
- The variety events which are simulated mostly within small ΔP at PCC in order to rich ANN with different possible cases, and most critical states.
- Detection time of the islanding cases is within IEEE 1547 standard, six voltage cycles time period (0.12 seconds) is very short time compared to 2 seconds.

- The proposed method in islanding detection can work properly inside the NDZ in case of low power mismatch on the PCC, without affecting the PQ like active detection methods.

5.3 Recommendations

- The proposed method can be used in PV inverters as effective islanding detector, simply by insertion the system parameters into the mathematical simulated model of this method.
- The ANN can be trained in different real systems according to privacy of every electrical network topology, components, and related system parameters.
- Since this kind of methods is not able to be tested over large grid-inverter real time operation, a similar small scale power system could be built to test, record, and simulate similar events. This would investigate the performance, and in force the validation of this approach.

5.4 Future Works

- For upcoming follow up of this research, it could be worthy to start the procedure by de-noising the voltage samples collected from the power system before inserting them into DWT. This may remove the common THD content in the signal, hence, it could reduce the ANN complexity and training time.
- While the DWT detail coefficients feature vector is the main factor used to train the ANN classifier, it is suggested for future work to investigate the correlation factors between the sub details with purpose to remove dependent details in order to reduce the ANN complexity and training time.
- As recent researchers recommend [26], especially in smart grids, islanding detection technique embedded inside inverter microcontroller chip should be more intelligent and flexible, the IDM should become adaptive with the grid topology, and conditions of operation. The tested grid in this study produced its own characteristic against islanding, this requires an IDM capable to adapt with the grid installation and could moderate itself continuously while the grid is upgrading.

References

[1] N. Sivakumar, M. Bansal, and S. Sahoo, “Islanding Issues of Grid-connected PV Systems,” *Int. J. Eng. Technol.*, vol. 5, pp. 726–733, 2013.

[2] L. Gao and J. Liu, “A review of islanding detection methods for photovoltaic generation system,” *International Journal of Multimedia and Ubiquitous Engineering*. 2016, doi: 10.14257/ijmue.2016.11.6.01.

[3] A. G. Abokhalil, A. B. Awan, and A. R. Al-Qawasmi, “Comparative study of passive and active islanding detection methods for PV grid-connected systems,” *Sustain.*, 2018, doi: 10.3390/su10061798.

[4] M. S. Kim, R. Haider, G. J. Cho, C. H. Kim, C. Y. Won, and J. S. Chai, “Comprehensive review of islanding detection methods for distributed generation systems,” *Energies*. 2019, doi: 10.3390/en12050837.

[5] T. Drizard, G. Diquerreau, and S. Vilbois, “Behaviour of PV inverters during islanding of a district,” in *CIRED - Open Access Proceedings Journal*, 2017, doi: 10.1049/oap-cired.2017.0786.

[6] I. Standards, C. Committee, D. Generation, and E. Storage, *IEEE Guide for Conducting Distribution Impact Studies for Distributed Resource Interconnection*. 2014.

[7] W. Y. T. Teoh and C. W. Tan, “An Overview of Islanding Detection Methods in Photovoltaic Systems,” *World Acad. Sci. Eng. Technol.*, 2011.

[8] R. de Castro Fernández and H. Rojas, “An overview of wavelet transforms application in power systems,” *Proc. 14th PSCC, Sevilla, Sess.*, 2002.

[9] Z. Mi and F. Wang, “Power equations and non-detection zone of passive islanding detection and protection method for grid connected photovoltaic generation system,” in *Proceedings of the 2009 Pacific-Asia Conference on Circuits, Communications and System, PACCS 2009*, 2009, doi: 10.1109/PACCS.2009.167.

[10] M. Ashour, L. Ben-Brahim, A. Gastli, N. Al-Emadi, and Y. Fayyad, “Matlab/Simulink implementation & simulation of islanding detection using passive methods,” in *2013 7th*

IEEE GCC Conference and Exhibition, GCC 2013, 2013, doi: 10.1109/IEEEGCC.2013.6705797.

[11] T. Sko??il, O. Gomis-Bellmunt, D. Montesinos-Miracle, S. Galceran-Arellano, and J. Rull-Duran, "Passive and active methods of islanding for PV systems," in *2009 13th European Conference on Power Electronics and Applications, EPE '09*, 2009.

[12] B. Mohammadpour, M. Zareie, S. Eren, and M. Pahlevani, "Stability analysis of the slip mode frequency shift islanding detection in single phase PV inverters," in *IEEE International Symposium on Industrial Electronics*, 2017, doi: 10.1109/ISIE.2017.8001361.

[13] B. Mohammadpour, M. Pahlevani, S. Makhdoomi Kaviri, and P. Jain, "Advanced slip mode frequency shift islanding detection method for single phase grid connected PV inverters," in *Conference Proceedings - IEEE Applied Power Electronics Conference and Exposition - APEC*, 2016, doi: 10.1109/APEC.2016.7467900.

[14] X. Chen and Y. Li, "An islanding detection algorithm for inverter-based distributed generation based on reactive power control," *IEEE Trans. Power Electron.*, 2014, doi: 10.1109/TPEL.2013.2284236.

[15] O. Arguence, F. Cadoux, B. Raison, and L. De Alvaro, "Non-detection zone of an anti-islanding protection with rate of change of frequency threshold," in *CIRED - Open Access Proceedings Journal*, 2017, doi: 10.1049/oap-cired.2017.0352.

[16] M. Zahran, Y. Atia, and M. M. Salem, "Active Anti-Islanding Based Inverter for PV Grid Connected System," *IPASJ Int. J. Electr. Eng.*, vol. Volume 2, pp. 17–35, 2014.

[17] A. R. Abdolabadi and H. R. Najafi, "A new islanding scheme based on multi-objective optimization for distribution systems implemented with DGs," in *2017 25th Iranian Conference on Electrical Engineering, ICEE 2017*, 2017, doi: 10.1109/IranianCEE.2017.7985238.

[18] S. Raza, H. Mokhlis, H. Arof, K. Naidu, J. A. Laghari, and A. S. M. Khairuddin, "Minimum-features-based ANN-PSO approach for islanding detection in distribution system," *IET Renew. Power Gener.*, 2016, doi: 10.1049/iet-rpg.2016.0080.

[19] U. D. Dwivedi and S. N. Singh, “Enhanced detection of power-quality events using intra and interscale dependencies of wavelet coefficients,” *IEEE Trans. Power Deliv.*, 2010, doi: 10.1109/TPWRD.2009.2027482.

[20] M. Heidari, G. Seifossadat, and M. Razaz, “An intelligence-based islanding detection method using DWT and ANN,” *Turkish J. Electr. Eng. Comput. Sci.*, 2015, doi: 10.3906/elk-1210-107.

[21] A. Graps, “An Introduction to Wavelets,” *IEEE Comput. Sci. Eng.*, vol. 2, no. 2, pp. 50–61, 1995, doi: 10.1109/99.388960.

[22] M. S. ElNozahy, E. F. El-Saadany, and M. M. A. Salama, “A robust wavelet-ANN based technique for islanding detection,” in *IEEE Power and Energy Society General Meeting*, 2011, doi: 10.1109/PES.2011.6039158.

[23] M. Hanif, U. D. Dwivedi, M. Basu, and K. Gaughan, “Wavelet based islanding detection of DC-AC inverter interfaced DG systems,” in *Proceedings of the Universities Power Engineering Conference*, 2010.

[24] V. L. Merlin, R. C. Santos, A. P. Grilo, J. C. M. Vieira, D. V. Coury, and M. Oleskovicz, “A new artificial neural network based method for islanding detection of distributed generators,” *Int. J. Electr. Power Energy Syst.*, 2016, doi: 10.1016/j.ijepes.2015.08.016.

[25] M. F. Møller, “A scaled conjugate gradient algorithm for fast supervised learning,” *Neural Networks*, 1993, doi: 10.1016/S0893-6080(05)80056-5.

[26] H. Laaksonen and P. Hovila, “Future-proof islanding detection schemes in Sundom Smart Grid,” in *CIRED - Open Access Proceedings Journal*, 2017, doi: 10.1049/oap-cired.2017.03.10.